Role of Lyotropic Liquid Crystals in Templating Mesosilica Materials

International Journal of Sciences

Research Article Volume 12 – July 2023 (07)

Role of Lyotropic Liquid Crystals in Templating Mesosilica Materials

Amelia Carolina Sparavigna[1]

[1]Department of Applied Science and Technology, Polytechnic University of Turin, Italy

Abstract: Here we consider the lyotropic liquid crystals and their role in templating the scaffolds of mesoporous silica materials. It was in 1992 that a Mobil Research group disclosed a method to produce silica particles having a regular network of pores with hexagonal and cubic symmetries. The method was proposed as a liquid-crystal 'templating' mechanism. Since the symmetries resulting in the silica scaffolds are those observed in the mesophases of lyotropic liquid crystals, the Mobil Research group supposed the presence of mesophases directly in the templating process. Here we discuss the method as it was reported in 1992 and what is today defined as the true or direct liquid-crystal templating LCT approach. It will be stressed that, in any case, LCT is a surfactant-assisted method that can be better defined as a supramolecular templating method. The template mainly happens in the form of a modified Stöber process. In this framework, the role of the curvature of silica-surfactant interfaces will be considered, the cubic phases of lyotropic liquid crystals analyzed in depth and the related surfaces with zero mean curvature discussed in detail.

Keywords: Liquid crystals, Lyotropic liquid crystals, Mesophases, Hexagonal phase, Curvature of interface, Cubic phases, Bicontinuous cubic phases, Mesoporous Silica Materials

1. Introduction

Liquid crystals (LCs) are soft matter materials possessing mesophases characterized by properties pertaining both to liquids and solid crystals (Chandrasekhar, 1992). The simplest example of mesophase is the nematic one. In it, calamitic molecules show a self-alignment of the long axes, whereas a positional order of their centers is lacking, being them randomly distributed. Consequently, a long-range directional order exists, described by the so-called nematic director field, but disorder remains in the molecular positions. Other sets of mesophases such as cholesteric, smectic, blue cubic, cubic, hexagonal, lamellar, and columnar phases had been identified and characterized in their intermediate state of order, usually by means of optical, thermal, and dielectric properties (Dierking, 2003; Demus & Richter, 1980). In some of the mesophases, the ordering of molecules can be easily altered by external stimuli; in this manner, LCs can be used to create systems which respond optically to electric fields such as in LC displays (Gray & Kelly, 1999), thermally to temperature as in thermometers (Doane et al., 1988), or chemically to molecular stimuli as in chemical sensors (Carlton et al., 2013). For active LC displays, thermotropic materials in nematic anisotropic phase are mainly used.

The liquid crystals are divided in the two main families of thermotropic (TLCs) and lyotropic materials (LLCs). Thermotropic substances exhibit mesophases as temperature is changed (Vertogen & De Jeu, 2012), whereas the lyotropic substances exhibit mesophases driven by concentration (Collings & Hird, 2017). In LLCs, the mesophases are formed under appropriate conditions of concentration of an amphiphilic mesogen (surfactant) dissolved in a suitable solvent. Besides temperature, LLCs have their composition that is inducing a larger variety of mesophases with respect to TLCs. For uses different from LC display applications, the consequent order transitions in LLCs are very attractive (Mezzenga et al., 2019). Applications include the generation of advanced materials, which are exploiting the topological properties of the hydrophilic / hydrophobic domains exhibited by LLC mesophases. Here we will consider the application of LLCs in what is defined the "liquid crystal templating" (LCT).

Using silica precursors or polymers, mesophases like those of the soft liquid crystals can be produced, obtaining unique geometrical surfaces frozen in solids. These solids, in particular the mesoporous silica materials (MSMs), are fundamental for applications ranging from pharmaceutical industry to energy storage (Giraldo et al., 2007; Li et al., 2012;

Published at: http://www.ijsciences.com/pub/issue/2023-07/
DOI: 10.18483/ijSci.2691; Online ISSN: 2305-3925; Print ISSN: 2410-4477

Amelia Carolina Sparavigna (Correspondence)
+

Wu et al., 2020). Mesoporous silica is a form of silica that possesses a mesoscale structure, with pores from 2 nm to 50 nm in diameter (porous materials have been IUPAC classified according to their pore sizes: microporous, less than 2 nm, mesoporous, from 2 nm to 50 nm, macroporous, greater than 50 nm; Fang et al., 2010). Pores of almost the same size are arranged regularly, being formed in the amorphous silica with a long-range order. The produced material is a rigid scaffold which can have the symmetry of mesophases observed in LLCs. The most common types of MSM particles have a hexagonal arrangement of long pores.

It was in 1992 that a publication disclosed an approach to obtain hexagonal mesoporous silica. The proposed approach was defined as a liquid-crystal 'templating' LCT mechanism. Here we will consider templated MSMs, to understand how LLCs are involved in them. We will see that a definition of this template mechanism is "surfactant-assisted synthesis", and that the produced mesoporous silica material is known as "micelle templated silica" material too. In the proposed discussion, we will consider both the mesophases frozen in the mesoporous silica materials and the mesophases of the lyotropic liquid crystals. The cubic phases in liquid crystals will be analyzed in depth. Besides the analysis of mesophases and LC templates, the proposed discussion aims to convey the general message that systems which are based on TLC, LLC, polymer, and silica materials can represent a fertile field for the study of future transformation technologies.

2. The first template

Mesoporous silica materials (MSMs) are rigid scaffolds exhibiting a regular arrangement of pores, in different space group symmetries, with the size of pores typically ranging from 2 to 50 nm. Besides being interesting by themselves (Bruckner et al., 2021), the range of applications where they are most relevant is incredibly wide. MSMs can be used as support material in catalysis (Liang et al., 2017), for energy storage (Li et al., 2016), as a host matrix for dyes (Huang et al., 2011), and for delivering biomedically active molecules (Bruckner et al., 2021). Moreover, MSMs can become hard templates to obtain carbon replicas (Kim et al., 2005).

MSMs produced by the so-called liquid crystal template (LCT) technique are generally viewed as the *inverted replicas* of a lyotropic liquid crystal phase, but the design of MSMs is requiring a deep knowledge of the template process, and this knowledge is still incomplete (Bruckner et al. 2021). However, it was in 1992, thirty years ago, that the "liquid crystal templating" was proposed. According to Nagaraj, 2020, the publications by a Mobil Research group (Kresge et al., 1992; Beck et al., 1992) represented a breakthrough in soft matter templating, triggering many investigations about mesoporous materials by LCT. The initial templating used a dilute solution regime in which the surfactant, on its own, was not able to form an LLC mesophase. In 1995, a method of 'true liquid crystal templating' (TLCT) was developed by Attard et al.; in this template the concentration of the surfactant was favorable for the formation of a liquid crystal phase on its own (Nagaraj, 2020). In TLCT the silica precursor was hydrolyzed and polymerized within the LC phase. TLCT allows the creation of mesoporous scaffolds having symmetries according to LC phase diagrams.

As told by publications of 1992, the aim of the Mobil Research group (Kresge et al., 1992: Beck et al., 1992) was that of obtaining a porous medium different from the typical microporous materials, which were structures with pores irregularly spaced and broadly distributed in size. Kresge and coworkers disclosed the synthesis of mesoporous solids from the calcination of aluminosilicate gels in the presence of a surfactant, stressing that the formation of MSM takes place by means of a liquid-crystal 'templating' mechanism, during which the silicate material forms inorganic walls between the ordered surfactant micelles.

According to Kresge and coworkers the production of silica particles with structured pores inside had been previously explored by Yanagisawa et al., 1990, who used single layered polysilicate kanemite to react with alkyl-trimethylammonium chloride solutions to form complexes of alkyl-

trimethylammonium and kanemite. During the organic intercalation, the SiO_2 layers in the complexes were condensed to form three-dimensional SiO_2 networks. The calcined products of the complexes had micropores 2–4 nm in diameter. The pore size was altered with the variation in the alkyl-chain length of the alkyl-trimethylammonium. The particles obtained in this manner are known as FSM-16. Kresge and coworkers, in 1992, mentioned the work by Yanagisawa et al. noting that the final product retains, in part, the layered nature of the precursor material.

In (Beck et al., 1992), the Mobil Research team presented the synthesis, characterization, and mechanism of formation of mesoporous molecular sieves named M41S. One member of the family named MCM-41 (Mobil Composition of Matter n.41) has a hexagonal arrangement of mesopores. It can be produced by means of different synthesis approaches. In (Beck et al., 1992), the authors stressed that microscopy and diffraction results obtained for MCM-41 are strikingly like those obtained from surfactant / water liquid crystals or micellar phases. As the source of silica, the researchers used sodium silicate, tetramethylammonium silicate and tetraethylorthosilicate (TEOS). The quaternary ammonium surfactant compounds were the cetrimonium (hexadecyl-trimethyl-ammonium) chloride and bromide (CTAB), that is cationic surfactants. In addition to the hexagonal MCM-41 class, other materials with different geometries have been synthesized by the Mobil Research group varying the surfactant to silicon mole ratio. For instance, when cetrimonium / silicon ratio is less than 1, the predominant structure is the hexagonal phase of MCM-41. As the ratio increases beyond 1, a cubic arrangement with space group *Ia3d* has been obtained. Today, this MSM having *Ia3d* space group is known as MCM-48.

In the synthesis of MSMs then, a sol–gel process goes from the hydrolysis to the condensation of the silica precursors in an aqueous solution of a surfactant, the concentration of which is often lower than that suitable to form the liquid crystalline phases (Gascón et al., 2016). The ordered mesophases appear due to the interaction between the silicate species in the solution and the external micellar surface, in a process based on a "cooperative self-assembly mechanism" according to Gascón et al., 2016, Wan & Zhao, 2007, Zholobenko et al., 2008, Huo et al., 1994. In the process, the silicate oligomers and the surfactant species influence each other during the polymerization leading to the growing of a liquid crystalline order. Interactions of organic parts with inorganic species are detailed by ALOthman, 2012. In the Figure 10 of the article by ALOthman, a schematic representation is given of the types of silica-surfactant interfaces.

In the article previously mentioned about TLCT method, Attard et al. observed that the templating mechanism proposed by Kresge, Beck and coworkers (1992), was a *cooperative process* that involved the interaction of inorganic ions with discrete surfactant aggregates. Attard et al. used in their experiments the liquid-crystalline phases of non-ionic surfactants such as octaethylene glycol monododecyl ether ($C_{12}EO_8$, EO represents ethylene oxide) and octaethylene glycol monohexadecyl ether ($C_{16}EO_8$), to template the silica. The liquid-crystalline behavior of the corresponding lyotropic mixtures had been previously studied in (Mitchell, 1983). Tetramethylorthosilicate (TMOS) was used as silica precursor. In this manner, the Hexagonal and Cubic Q^{230} (space group *Ia3d*) mesophases were the templates. Contemporary to the work by Attard et al., non-ionic polyethylene oxide (PEO) surfactants in dilute concentration have been used for templating the silica by Bagshaw et al., 1995.

Be a cooperative process or an LCT, Niculescu (2020) asserts that it was in 1992 that the first surfactant-assisted synthesis of MCM-41 mesoporous silica was achieved. In 2001, MCM-41 MSMs begun to be studied for bio-applications as a matrix for drugs release, and since then, extensive research was devoted to improving MSM in biomedical applications (see Niculescu and references therein). Let us remember that also MCM-48 had been produced at the same time MCM-41 had been prepared.

In the recent publication by Bruckner et al., 2021, the TLCT is properly defined as a “direct liquid crystal

templating", in contrast to the general "liquid crystal templating," originally proposed in 1992. In the *direct* LCT, the surfactant solutions are much more concentrated and form LLC phases in the binary water/surfactant systems. In (Bruckner et al., 2021) it is told that the beauty of this method is coming from the broad already existing knowledge of the properties of LLC phases, and from the possibility of investigating new systems with relatively little effort. Bruckner and coworkers demonstrated by their investigation that "TLCT indeed exists", because the initially isotropic mixture turns, after some time, into an intermediary LLC with colloidal silica as a continuous phase. The success of the templating process is due to this "intermediary formed liquid crystal phase", fully developed before the solidification of the material. The surfactant used for experiments is the triblock-co-polymer Pluronic P123, "which enjoys high popularity for the fabrication of MSMs".

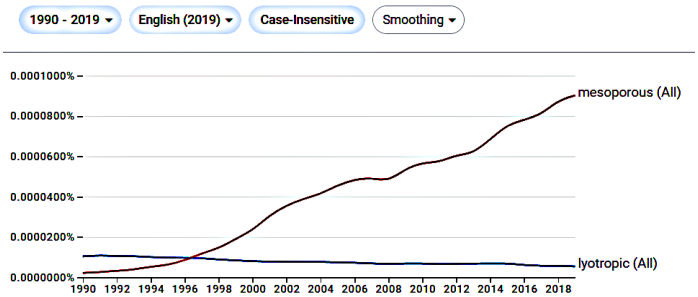

Figure 1 - The role of the disclosure by Mobil researchers in 1992 about mesoporous silica materials is also evidenced by the Google Books Ngram Viewer. This is an online search Google engine that charts the frequencies of any set of search strings, in printed sources published between 1500 and 2019. Ngram Viewer can search for a word or a phrase.

3. Notation convention of space groups

Previously, we have mentioned the space group *Ia3d* for MCM-48. *Ia3d* is a notation largely used for this and other materials (see for instance, Vallet-Regí et al., 2022, Kleitz et al., 2003, Paccamiccio et al., 2006). Let us shortly discuss the notation. First, we must note that the "space group" refers to the complete description of three-dimensional crystal symmetries.

One of the commonly used conventions to indicate the 230 space groups in three dimensions is that which is known as the Hermann-Mauguin notation. It uses four symbols. The first symbol is a letter (*P*, *I*, *R*, *F*, *A*, *B*, or *C*) referring to the Bravais lattice type. These letters mean: *P* Primitive, *I* Body centered (German "Innenzentriert"), *F* Face centered (German "Flächenzentriert"), *A* Base centered on A faces only, B Base centered on B faces only, *C* Base centered on C faces only, *R* Rhombohedral. In the case of *Ia3d*, *I* means that its Bravais lattice type is *I*, body-centered, with lattice points on the cell corners, with one additional point at the center of the cell, that is Innenzentriert.

In the Hermann-Mauguin notation, the three letters following the one related to the Bravais lattice refer to the point group of the crystal. Some modifications to the notation are used for keyboard; for instance, a bar above a number is entered with a minus sign. The second, third and fourth symbols in the Hermann-Mauguin notation are referring to the primary, secondary, and tertiary symmetry directions. Letters *a*, *b*, and *c* are indicating a glide-plane symmetry operation due to a reflection associated to a translation, *t*, parallel to the plane. In the case *a*, *b*, *c*, the translations are parallel to the corresponding lattice vectors ($t=a/2$, $t=b/2$, $t=c/2$). Letters *n* and *d* refer to 1/2 and to 1/4 translations parallel to the diagonal plane. The *d* glide-plane is also known as the *diamond glide*. Rotation axes are denoted by an integer number n, that is 1, 2, 3, 4, 5, 6, 7, 8 ... (angle of rotation $\varphi = 360°/n$). The symbol $\bar{n}$ is used for an n-fold rotoinversion, that is a rotation by an angle of 360°/n with inversion. $\bar{2}$ is equivalent to a mirror plane and usually notated as *m*.

In *Ia3d*, the secondary symmetry direction is denoted by the number 3. However, of *Ia3d* space group different notations exist in literature: *Ia-3d* or $Ia\bar{3}d$

(see for instance, Neto & Salinas, 2005, Miyasaka et al., 2012). Let us stress that the minus sign is often entered instead of the bar above the number. The Hermann-Mauguin correct notation used by Neto and Salinas in their book on lyotropic liquid crystals ($Ia\bar{3}d$) indicates a rotoinversion axis (an axis combining rotation and inversion). However, here we will continue to use the notation *Ia3d* , which is mainly used for mesoporous silica materials but also for the liquid crystal mesophases. The same we will do for the other cubic mesophases mentioned in this review.

4. Two pathways

In the discussion of controllable approaches to the formation of mesoporous silicates, Wan and Zhao, 2007, are proposing in their Figure 1 a cartoon with two pathways for the mesosilica synthesis processes, that the authors are defining as "cooperative self-assembly" process and TLCT process. The same cartoon is given by Lagerwall and Scalia (2012), in their discussion of a new era for the liquid crystal research.

In the pathway A, that is the cooperative self-assembling, we start from a liquid solution with separated micelles, surfactant molecules in solution and inorganic species (generally, it is used a solution in water of surfactants, which can be classified in cationic, anionic, and nonionic surfactants). Then, with a cooperative nucleation, micelles are surrounded by inorganic species. In the following cooperative aggregation and phase separation, the liquid becomes a mixture of solution and precipitation, where micelles tend to arrange themselves in a specific geometry (the Figure 1 in Wan & Zhao is displaying hexagonal geometry; actually, the authors are modeling MCM-41 template). In the mixture, we have the liquid crystal formation with molecular inorganics. A further polymerization and condensation of inorganics is obtained by the elimination of the template. In the review by Wan and Zhao a detailed discussion of the interactions between organic and inorganic materials is given too. The cooperative assembly is given as a process driven by weak noncovalent bonds (hydrogen bonds, van der Waals forces, electrovalent bonds).

The following cartoon is illustrating the pathway A as proposed by Wan and Zhao. We will consider this pathway again, when we will illustrate the work by Alfredsson and Wennerström, 2015. The researchers were able to identify several steps in the templating process of mesosilica with hexagonal arrangement of cylindrical pores.

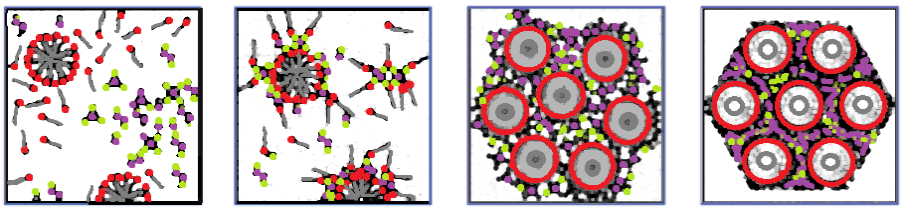

Figure 2 - a cartoon according to that proposed by Wan and Zhao to illustrate the pathway A. From left to right: liquid solution with micelles, surfactant molecules (red heads and gray tails) and inorganic species (violet and green); micelles surrounded by the inorganic species; micelles arranged in a quasi-hexagonal geometry; condensation of inorganic silica around the surfactant.

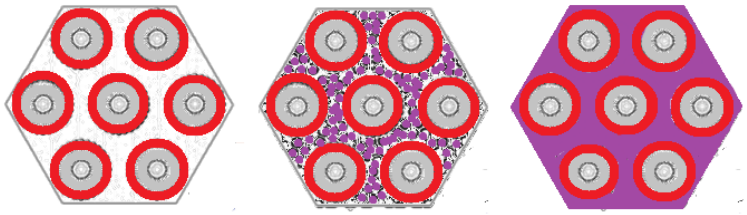

Figure 3 - Another cartoon according to Wan and Zhao to illustrate pathway B. From left to right: liquid crystal in the Type I Hexagonal phase; inorganic species (violet) in the water surrounding the micelles; condensation of inorganic silica around the surfactant.

In the pathway B, that is the direct LCT, we start from the liquid crystal formation. In the liquid crystal it is incorporated the inorganic precursor. The precursor is transformed in the desired material and then the template is eliminated. For what concerns the process proposed by Attard and coworkers, Wan and Zhao note that the condensation of the silica precursor is improved due to the confinement around the surfactant and that a ceramic-like framework is formed. For pathway B, a similar simplified sketch is given in the article by Bruckner et al., 2021, where it is told that the mixing of surfactant and water in specific proportions creates an LLC mesophase. In the sketches of Wan & Zhao and Bruckner et al., it is shown the hexagonal mesophase, specifically the normal Type I Hexagonal phase. A silica precursor is added in the aqueous part of the LLC mesophase, and it starts to condensate around the micelles, creating a hybrid material with silica and surfactant. In the direct LCT, being the silica condensed in the water part of the LC mesophase, the resulting structure is the inverted replica of the original mesophase. In the case of the normal Type I Hexagonal phase, it is the reverse Type II Hexagonal scaffold (when we will discuss the lyotropic mesophases we will specify the nomenclature).

To obtain the porosity in the material we need the removal of templates. As noted by Wan and Zhao the different removal methods which are applied to the material are influencing the features of the mesoporous silicas. The commonly used method is the calcination. The method is easy to operate. The organic surfactants are decomposed or oxidized in air atmosphere. It is important to control the temperature programming rate to prevent the collapse of the silica. Other methods for the extraction of the organic template are discussed by the given review.

5. Pathway A

Let us consider a cationic surfactant. As told by Wan and Zhao, the silicate polyanions, which are in the form of silicate oligomers in the liquid solution, are interacting with the positively charged heads of the surfactant, because of the Coulomb interaction. At the interface, the silicate species polymerize with a further change of the charge density of the silica layers. As the reaction goes on, the supramolecular arrangement of the surfactant molecules and the charge density at the interface influence each other. What is governing the assembly process of the hybrid material, as told by Wan and Zhao, is the matching of charge density at the interface. Then, the mesophase of the hybrid material is that possessing the lowest interface energy. After reporting about the transformation of the isotropic micellar solution mesophases when mixed with anionic silicate oligomers, Wan and Zhao are also discussing the cooperative formation mechanism in the case of a nonionic surfactant liquid, investigated by in situ techniques in Ruthstein et al., 2003, 2006. These researchers studied the formation of the mesoporous silica known as SBA-15. Ruthstein and coworkers observed a continuous transformation of the spheroidal micelles changing into threadlike micelles. Bundles of these micelles were formed, arranged as in the final material.

Wan and Zhao illustrate several other investigations based on the interaction at the surfactant / inorganic species interface. They are also reporting that Monnier et al., 1993, and Huo et al., 1994, gave an expression for the free energy, containing the contribution of the interaction between inorganic silica and surfactant, the free energy for the inorganic material, the contributions of the van der Waals force and conformational energy of the surfactant, and the chemical potential of the species in solution phase.

6. Pathway B

In illustrating the pathway B, that is the direct LCT, we used as a model a sketch in Wan & Zhao and in Bruckner et al., 2021. In the caption of the Figure 1 of this last reference, it is clearly told that it is a "simplified sketch" of a TLCT process. And it is also told that “an added silica precursor ... , dissolves in the aqueous part of the LLC, starts to polycondensate around the micelles”, and, in this manner, it is formed a hybrid material of inorganic silica and organic surfactant. However further discussion is necessary and we will help us with the article by Bruckner et al. about the “true” or “direct” LCT.

Bruckner and coworkers remember that Attard et al., 1995, used a hexagonal (H_1, that is Type I hexagonal) LLC phase for the templating. "When they added the

silica precursor", in the form of the tetramethyl-orthosilicate (TMOS), "the mixture initially turned into an isotropic fluid". The birefringent phase, that is the hexagonal one, "could be recovered" removing the methanol formed during the TMOS hydrolysis. The following discussion, in the article by Bruckner et al., tells that it was a study by means of deuterium NMR spectroscopy that investigated the change from the isotropic to the ordered hexagonal structure (Attard et. al., 1998). In the article published in 1998, Attard et al. told that the hydrolysis of TMOS in the mixture of surfactant and water "occurs rapidly", yielding an *isotropic liquid*. The reason is in the fact that the "methanol, formed during the hydrolysis step, *destroys the mesophase*." As previously told, the removal of methanol in vacuum "restores the original mesophase". Therefore, as noted by Bruckner et al., Attard and coworkers suggested that the isotropic solution turns into an LC, in a conversion which re-creates the initial birefringent order. The conclusive suggestion is that a hybrid material can be *predicted* according to the base LLC phase diagram, in the case that the *water* volume fraction is replaced by "the *same* volume fraction of inorganic material".

Then the pathway B in the Fig.3, the same shown by Wan & Zhao and Bruckner et al., is "simplified" because the insertion of silicates is destroying the hexagonal mesophase, which is formed again in the new hybrid material. Therefore, we have an intermediate phase with isotropic order in the mixture. In this case, the pathway B can be seen as in the following Fig.4.

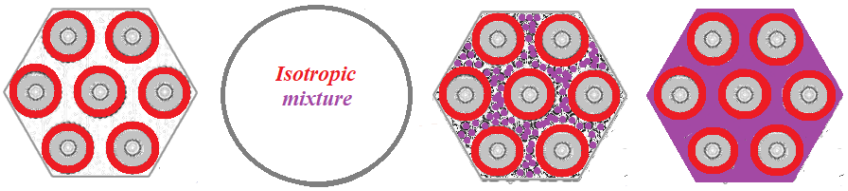

Figure 4 - In the pathway given by Attard et al. and by Bruchner et al., the hexagonal inorganic-organic mixture is coming from an isotropic mixture, observed after the silica precursor is added to the LLC. From left to right: liquid crystal in the Type I Hexagonal phase; isotropic mixture; inorganic species (violet) in the water surrounding the micelles; condensation of inorganic silica around the surfactant.

Bruckner investigated different LLC mesophases with the triblock-copolymer Pluronic 123 in water. When the silica precursor is added, the researchers observed the formation of isotropic mixtures for the hexagonal H_1 and cubic I_1 phases. But the behavior is different in the case of the lamellar L_α phase: the evolution of the system given by SAXS patterns tells that "immediately after mixing" organic and inorganic materials, "the clear fluid showed a sharp peak ... which proves that an L_α phase is formed" in the mixture. This behavior is ascribed to the viscosity of the lamellar phase. Then, an isotropic mixture is not observed.

We have mentioned before MCM-41 (hexagonal), MCM-48 (*Ia3d* cubic), and here we have another material with a lamellar geometry, and we have the lamellar MCM-50 too. The genesis of these three materials has been investigated by means of Molecular Dynamics simulations (Chien et al., 2017). Expanding some previous works (Pérez-Sánchez et al., 2013, 2016) that simulated the mesosilica formation at low surfactant concentration, Chien and coworkers in 2017 analyzed the formation of silica mesoporous materials in the presence of higher surfactant concentrations. The researchers are reporting good agreement with experimental observations, concluding that the model suggests the formation of MCM-41 through a cooperative templating mechanism and not in an LCT mechanism. Moreover, Chien and coworkers add that their results "suggest that the LCT mechanism is not compatible" in the case of MCM-48 materials, but the researchers "cannot rule out this mechanism in the synthesis of MCM-50 at very high surfactant concentrations".

The experimental investigations by Bruckner et al. are more recent than the mentioned simulations by Chien et al. and are showing an LC template mechanism for the lamellar structure, without the presence of an isotropic mixture. In the lyotropic

liquid crystals, the lamellar L_α phase appears at concentration of amphiphile higher than that of the hexagonal H_I and of the cubic (Type I) phases. Let us consider an "inverted" hexagonal H_{II} mesophase, where the gray tails of the surfactant are outside the red shell of the molecular heads (that is, with an inverted representation of Fig.4). Water is filling cylinders arranged in hexagonal geometry. In templating this LLC phase, we could have silica rods in hexagonal arrangement. Of course, this is not a mesoporous silica, and it is difficult to find somebody templating an "inverse" liquid crystal, - in fact, in Huang et al., 2002, we can find cuprite nanowires obtained by electrodeposition from a "reverse" (or "inverse") hexagonal liquid crystal mesophase - but it could be interesting to find whether the template could occur in a pathway as that observed for the lamellar phase or not. The "inverse" of the mesoporous structure of the MSMs is that displayed by their carbon replicas (see the scheme n.1 in Janus et al., 2022).

7. Open pores

In the introduction of the review by Wan and Zhao, it is stressed that the synthesis of mesoporous molecular sieves is producing "open framework structures", that is structures with pores that are open and not capped. In this manner, the open framework grants the access to the mesoporous silica material to the desired load, metal ions and reagents. This is the fundamental feature for application in "the fields of catalysis, sensors, electronic devices, biology, nanodevices, separation, etc" (Wan and Zhao).

However, why are the pores open? We can find the answer in the dissertation by Emma Johansson, 2010. It is told that the theoretical analysis of the formation of MSMs revealed that a silicate "preferably adsorbs onto low curvature sections of the micelles". We have seen before that the spheroidal micelles are changing into elongated threadlike micelles. During the elongation, "the surface energy of the spherical caps on the ends increases" and consequently silicates avoid them, "leaving the pore ends open in the calcinated material".

Emma Johansson is mentioning the work by Gov et al., 2006. In this article, in a schematic view of the mechanism which is forcing the micelles to elongate after the addition of silicate ions, we can find the adsorption of these ions onto the surfactant headgroups, adsorption which is reducing the spontaneous curvature of the surfactant layer. Moreover, the adsorbed silicate is inducing an attractive interaction between micelles. Consequently, the set of spherical micelles become an assembly of cylindrical surfactant structures surrounded by silicates.

About the open access to mesopores, let us report some sentences from Eftekhari & Fan, (2017), that are discussing the ordered mesoporous carbon. "In the material characterization, the mesopores might seem open in TEM images, but when packing the particles, some mesopores are blocked by the neighboring particles". Therefore, the material performance is depending on the accessibility of pores which is also determined by the assembly of particles. And this is true also for silicas.

8. Evolution

In the work by Ruthstein et al., 2006, that we have previously mentioned, it was shown the evolution of structures which are present in the solution used to obtain the hexagonal mesoporous material SBA-15 (analogous to MCM-41). The experimental study used the direct imaging and freeze-fracture replication cryo-TEM. The method was that of sampling the reaction mixture at different times, after the addition of tetramethoxyorthosilane to the solution of Pluronic P123 (temperature 50 °C). The sequence of micrographs indicated that the solution was initially containing spheroidal micelles. Then, as previously told, the micelles evolved into threadlike micelles. Passing time, the micelles became longer and straighter. Bundles then appeared, but the hexagonal arrangement was shown only when the solution started to precipitate (at a time of 40 min). To observe the structures after 40 min, the freeze-fracture replication was carried out as well (about the freeze-fracture electron microscopy, see the article by Severs, 2007). The researchers used the same reaction conditions of previous in situ EPR experiments. In this manner, Ruthstein and coworkers were able to correlate the molecular level events with the shape evolution of the

microstructures. The experiments evidenced that "the elongation of the micelles is a consequence of a reduction of the polarity and the water content within the micelles due to silicate adsorption and polymerization".

Let us consider that the polymeric micelles, composed of amphiphilic block copolymers, are characterized like core–shell structures, that is a hydrophobic core and a hydrophilic shell, which is giving stability to the micelle. However, the micellar structure is also depicted as a core-shell-corona assembly, and the corona serves as the template (Sasidharan & Nakashima, 2014). In the case of triblock-copolymer Pluronic P123 ($EO_{20}PO_{70}EO_{20}$), that is PEO-PPO-PEO, the micelle is given as in the following cartoon (Luo et al., 2019).

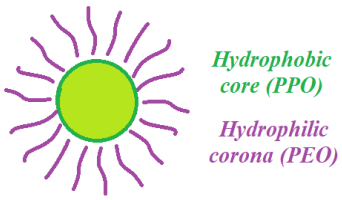

Figure 5 Ruthstein and coworkers noted that, during the time evolution, there is a decrease of the polarity and water content of the core / corona interface.

9. Soft templating

As illustrated by Wu et al., 2020, wide ranges of methods exist to prepare structured porous materials. The Figure 1 of the given reference summarizes the methods dividing them into three main families: soft templating, hard templating, and template-free method. The preparation of materials by templating methods, both soft and hard, can tune the pore sizes in a specifically designed shape, but these methods require a removal process, to free the templated scaffold from templating agents. The template-free methods are driven by spontaneous formation phenomena and self-assembly processes. They are simpler methods, but difficult to control.

In Wu et al., 2020, the soft templating method is defined as referring to the use of molecular systems possessing some organization structure. The authors are introducing three major soft templating methods: surfactant templating, emulsion templating and breath-figure templating. The surfactant templating is the family of methods to which LCT belongs (actually, LCT and TLCT methods are nested into the surfactant templating methods, nested into the family of soft templating methods). The surfactant method uses molecular aggregates (micelles, liquid crystals, vesicles, etc.) formed by surfactant molecules. As illustrated in the review by Wan and Zhao, through their relevant interactions, the aggregates are the agents driving the templating process. The structured porous materials are including silicon dioxides, metals, and metal oxides (see Wu et al., 2020, and references therein). Being generally the surfactant molecules some organic molecules, the in-situ carbonization of them can enhance the conductivity of final scaffold, “making this method an important tool in the field of energy storage” (Wu et al., 2020). The review by Wu and coworkers, 2020, is regarding the hierarchically structured porous materials. The materials are exhibiting a hierarchy of the pore size, so that in them we can find micro-, meso- and macropores. These structures are used in catalysis, photocatalysis, adsorption, separation, energy conversion and storage (see the references given by Wu et al.). As stressed by the authors of the review, the materials are featuring different levels of porosity, characterized by a pore regularity at each level, with interconnection between each level of porosity. In these materials, the access to a volume with relevant porosity and high surface area facilitates the transport of electron / ion and the diffusion of mass. These characteristics are relevant for the energy storage technology (Wu et al., 2020, Sun et al., 2016, Li et al, 2012).

10. Modified Stöber process

Among the templating methods for silicas, we can find the Stöber process and its modifications (Niculescu, 2020). Werner Stöber and his team proposed a method to prepare silica particles of controllable and uniform size in 1968. In their process, a molecular silica precursor, such as tetraethylorthosilicate, first reacts with water in an alcoholic solution. The resulting silicic acid molecules are building the final silica particles as spheres. The developed system of chemical reactions was able to control the growth of silica particles of

uniform size. Ammonia was used as a morphological catalyst.

Soon after, some patents had been applied to modify the method to have silica spheres with hollows inside. Among them, we find the patent by Chiola et al., applied in 1969 and approved in 1971. In it, we can find described an improvement for producing silica from tetra-alkylsilicate in the presence of cationic surface-active agents. We find that TEOS and surfactant CTAC (cetyl-trimethyl-ammonium chloride) were used in an example. In 1997, Di Renzo et al. repeated the synthesis described in the patent obtaining highly ordered hexagonal MSM, that is a mesoporous silica material having the properties of MCM-41 (Xu et al., 2009). In their work, Di Renzo and coworkers observed that Ralph K. Iler had already reported in his book of the patent by Chiola et al., but stressing that this patent does not give the characterization of the precipitation product beyond its bulk density. Mentioning Huo et al., 1994, Di Renzo et al. are adding that the "low-density material of Chiola et al. is not only a forerunner of MCM-41 silica, but also of surfactant-templated materials of different composition".

In another publication of 1997, Grün et al. discussed a modified Stöber process to have spherical porous particles. The researchers noted that MCM-41 material obtained by the classical procedure of Beck et al., 1992, yields loose agglomerates consisting of a wide particle size distribution. However, the control of the particle morphology of MCM-41, which can provide the synthesis of beads of defined size, "could open up new possibilities for the application of MCM-41 as a packing material in chromatography or as an easy-to-handle form of MCM-41 for catalytic purposes". Grün and coworkers stressed that in 1997, only hexagonal prisms of MCM-41 have been reported in the literature, and therefore their communication was describing the first synthesis of spherical silica particles featuring an MCM-41 structure. It is told that "the synthesis procedure itself is a *modification of Stöber's well-known synthesis* of monodisperse silica spheres". The researchers modified Stöber process by adding a cationic surfactant to the reaction mixture, thus providing a source of micelles. Again, the n-hexadecyl-trimethyl-ammonium bromide and n-hexadecyl-pyridinium chloride were used as cationic surfactants, while ethanol was chosen as the solvent and tetraethoxysilane (TEOS) served as the silica source. Aqueous ammonia was used as a catalyst.

In 1999 and 2000, another modified Stöber process was proposed for the controlled formation of silica spherical particles (Boissière et al., 1999, 2000). In Boissière et al. we can find mentioned, at the beginning of the article, among the "micelle templated structures" (MTS) the mesoporous alumino-silicates M41S. It is told that since their discovery, research has succeeded in expanding the use of ionic surfactants. Moreover, the article is pointing out that the use of non-ionic surfactants such as those based on polyethylene oxide and block-copolymers produced a whole family of mesoporous silicas named as MSU-V, MSU-G and MSU-X. In the last silicas, X refers to some non-ionic surfactant molecules (see please the given reference for details). The synthesis proposed by Boissière et al. is based on a sodium fluoride aided hydrolysis of tetraethoxysilane. The mixture is dissolved into a dilute solution of non-ionic polyethylene oxide-based surfactants. The researchers modified the synthesis process, asserting that the changes they have introduced drastically influenced the result of the preparation. The main feature of their approach lies in the possibility of discriminating the hydrolysis and assembly steps in the synthesis of the particles. To this purpose, the researchers added an intermediate step where a mild acidic medium was used. During this step it was observed a stable colorless microemulsion, containing all the reactants. Accordingly, the researchers concluded that a homogeneity at molecular level was achieved before the start of the reaction.

Let us note that in (Liu et al., 2006), the method proposed by (Kresge et al., 1992) has been assigned as a "modified Stöber method" tout court. It is also necessary to add that, in 1997, Lüdtke et al. obtained porous silica spherical beads to be used in chromatography, again with a modified Stöber method. To induce an inner particle porosity of the Stöber beads, the researchers modified the procedure in such a way to use n-alkyl-trimethoxysilane as an

additive to the starting reaction solution (as disclosed by Kaiser and Unger in the Patent Application No. P19530031.9, 1995). The final product is an organosilica composite, where we can find n-alkyl groups in its volume. To produce the porosity inside the particles, the beads are subjected to calcination. During calcination, the organic alkyl chains are removed. Lüdtke et al. are consequently asserting that using n-alkyl-trimethoxy-silane as porogene and by adjusting the relative content of tetraethoxysilane in the starting solution, it is possible to control the pore structure of the beads.

Since some silica precursors had been previously mentioned, let us suggest the article by Karamikamkar et al., 2020, where it is possible to find a list of several of them, used in the framework of the production of aerogels. Some n-alkyltrimethoxysilane coupling agents are given in Nakazumi and Hara (2017).

11. The surface

We have seen that it was thirty years ago that the "liquid-crystal templating" was proposed and the MSMs popularized. But, as already asserted by Niculescu (2020), it was in 2001 that MCM-41 MSMs begun to be considered for bio-medical applications. Of 2022 it is a review (Vallet-Regí et al., 2022) which is giving a detailed description of MSMs as drug delivery systems, besides mentioning the chronology of the events regarding the syntheses of mesoporous materials (LCTs, TLCTs, modified Stöber processes as in Niculescu, 2020). It is stressed once more the fact that it took about ten years to find the mesoporous materials mentioned as drug delivery tools, the first time right in an article by Vallet-Regí and coworkers, 2001.

In the review of 2022, we can find some of the features of MSMs that are relevant for drug delivery. One is the homogeneity of the porous size, which allows the possibility to control the load and release of drugs. Another characteristic, which is regarding the surface of the silica, is its content of silanol groups that, according to Vallet-Regí et al., 2022, can be modified to obtain a better control of the material in the drug delivery.

In (Zhao et al., 1997) a comprehensive study of the surface chemistry of MCM-41 is given. The spectroscopic investigation found three types of silanol groups, which are: single, $(SiO)_3Si{-}OH$, hydrogen-bonded, $(SiO)_3Si{-}OH\text{-}OH{-}Si(SiO)_3$, and geminal, $(SiO)_2Si(OH)_2$. The number of silanol groups on the surface is depending on the method used for the template removal. The researchers pointed out that the free silanol groups - single and geminal silanols - are those which are easily accessible for processes of silylation, which are used to modify "both the physical and chemical properties of MCM-41". From the article, it seems that the "physical" property is related to the physically adsorbed water.

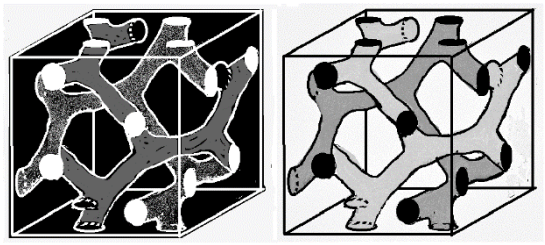

Figure 6 - On the left, grey color represents the walls of the pores in silica (black). White represents the section of the pores when they cross the faces of the cubic unit cell. On the right, the characteristic pore system of KIT-6 (see Van Der Voort et al., 1998; in the given reference it is told that the structure is consistent with the model of cubic phase Q^{230} proposed by Mariani et al., 1988, for water - surfactant systems).

12. Cubic KIT-6 and KIT-5

As previously told, in 1992 MCM-48 MSM had been produced having cubic *Ia3d* symmetry. Today, another MSM family with space group *Ia3d* is known as KIT-6. These materials were first synthesized by Ryong Ryoo's research group of the Korea Advanced Institute of Science and Technology in 2003 (Kleitz et al., 2003). The regular structure is characterized by

a 3D two independent interpenetrating arrangements of mesopores (see Fig.6), analogous to those observed in the structure of MCM-48 material, but with larger pore sizes, besides possessing a high hydrothermal stability (Wawrzyńczak et al., 2022). The KIT-6 network of channels can provide easy access and diffusion for different molecules in the channels without blocking them (Wawrzyńczak et al., 2022).

As we will see during the discussion of the cubic phases of LLCs, and as stressed in 2022 by Vallet-Regí et al. for the similar MCM-48, the two independent pore systems of the *Ia3d* cubic structure are separated by a gyroid minimal surface. This minimal surface has a zero mean curvature and a saddle splay (negative Gaussian) curvature. For what concerns the surface of the pores and the presence of silanol groups, they have been considered by Basso et al., 2020, that studied the concentration of the groups, relevant when the material is used for adsorption.

In 2005, the Ryong Ryoo's group announced the production of MCM-48-like large mesoporous silicas via a *facile* synthesis by means of a ternary triblock-copolymer butanol-water system (Kim et al., 2005). As shown by the research, the cubic phase domain is *remarkably extended* by controlling the amounts of butanol and silica source correspondingly. The extended phase domain leads to *facile* synthesis of the cubic *Ia3d*. These cubic materials possess high specific surface areas, high pore volumes, and tunable pore diameters in narrow distribution of sizes ranging from 4 to 12 nm. The authors also studied the carbon replicas, using sucrose as the carbon precursor, stressing that they obtained either the same *Ia3d* structure or *I41/a* (or lower symmetry), depending on the controlled synthesis conditions for silica.

Kim et al., 2005, provide details to prepare the mesostructured silica materials using a mixture of poly-(alkylene-oxide)-based triblock-copolymer Pluronic P123 ($EO_{20}PO_{70}EO_{20}$) and n-butanol. The silica source was tetra-ethyl-ortho-silicate TEOS or sodium silicate. The molar composition of the starting reaction mixture was given by P123, TEOS, BuOH, HCl and H_2O (see more detail of the method in the given reference).

The *facile* synthesis is also used by Wawrzyńczak et al., 2022, where the researchers reported their synthesis route of KIT-6 with commercially available P123–butanol mixture in aqueous solution. By Wawrzyńczak et al., 2022, it is stressed that the structure can be used as a template to fabricate successfully bicontinuous arrays of nanotube-type carbon, the CMK-9 mesoporous carbon, as well as rod-type, the CMK-8. CMK means Carbon Mesostructured by KAIST, Korea Advanced Institute of Science & Technology.

Pluronic P123 is a symmetric triblock-copolymer comprising poly-ethylene-oxide (PEO) and poly-propylene-oxide (PPO) in an alternating linear fashion, PEO-PPO-PEO. In the copolymer we have the hydrophilic ethylene oxide and the hydrophobic propylene oxide, then Pluronics have an amphiphilic structure (Shirwaiker et al., 2014). Pluronic is also known as Poloxamer 407. And, because of their amphiphilic characteristics, that is the presence of hydrophobic and hydrophilic components, pluronics have surfactant properties so that they can interact with hydrophobic surfaces and biological membranes (Bearat & Vernon, 2011). In the same reference it is told that, being the material amphiphilic, the individual block copolymers, which are known as unimers, can form micelles in aqueous solutions. If the concentration of unimers is below that of critical micelle concentration (CMC), unimers remain as a molecular solution in water. As the concentration is increased above CMC, unimers self-assemble and form micelles, displaying spherical, rod-shaped or lamellar geometries.

Have we a TLCT process? It is not easy to answer. However, we have for sure a surfactant-assisted process. In any case, Pluronic P123 is an LLC material (and we have found it at the beginning of our discussion when we have mentioned the work by Bruckner et al).

In (Zhang et al., 2008), the researchers have observed lyotropic liquid-crystalline phases formed by P123 in ethyl-ammonium nitrate (EAN). The lyotropic

mesophases which are displayed at 25 °C are: normal micellar cubic, normal hexagonal, lamellar, and reverse bicontinuous cubic. The mesophases have been identified by means of the polarized light optical microscopy and small-angle X-ray scattering measurements.

As told by Chen et al., 2012, in the aqueous system the phase behavior of P123 was very similar to that in EAN with the *Fm3m* I_1 cubic phase appearing at 30 wt%, as previously reported in the literature (Soni et al., 2006). Being the $(EO)_{20}$ head group of P123 considerably larger than that of other amphiphiles, it is observed an increase of the curvature which is promoting the formation of cubic phase in EAN and water (Chen et al., 2012). The lamellar phase was formed at lower concentrations in water compared to EAN. This experimental result tells that the phases formed in water are shifted towards lower concentration regions. Let us stress also that P123 forms lyotropic phases at room temperature.

The *Fm3m* cubic phase is a cubic close-packed structure where spherical micelles are assembled (see Aleandri & Mezzenga, 2020, for a picture of the inverse *Fm3m* phase and other lyotropic phases). Let us remember that *F* means face centered, Flächenzentriert. In 2003, Kleitz et al. disclosed the synthesis of a large cage face-centered-cubic *Fm3m* mesoporous silica. The name of this material is KIT-5. The cubic *Fm3m* symmetry has been determined by powder X-ray diffraction (XRD) and transmission electron microscopy (TEM) analyses. The calcined samples are providing large cages made of silica. The method to produce this material is based on an aqueous synthesis involving the use of Triblock Copolymer F127 at low HCl concentrations. The application of hydrothermal treatments, with temperatures ranging from 45 to 150 °C, produces different mesopore diameters and apertures. Using KIT-5, in 2005, Vinu et al. produced cage type mesoporous carbon, that is a "carbon nanocage".

13. MCM, KIT, SBA, FDU, MSU et al.

MCM-48 and KIT-6 have the same cubic group *Ia3d*, but they have been originated from different LCT materials. Moreover, the materials can be subjected to different calcination processes and, consequently, have different silanol groups on the surfaces of the pores. The same is true for other geometries of MSMs. We can find hexagonal MCM-41 and hexagonal SBA-15, a mesoporous silica sieve developed by researchers at the University of California, Santa Barbara. Mesoporous silica SBA-15 is synthesized using Pluronic P-123 and tetraethoxysilane (TEOS) for the source of silica. Again, we have the same symmetry of MSMs, templated with different products.

The discovery of SBA-15 is ascribed to the Galen D. Stucky Group in 1998 (Zhao et al., 1998). SBA-15 has a high specific surface area in a final material which is stable and displaying a high mechanical resistance (Galarneau et al., 2007, Benamor et al., 2012). In Roucher et al., 2019, it is stressed that the main feature of the materials is the presence of quite large pores, with respect to zeolites, which is consequently allowing even large molecules to diffuse. In the discussion by Vallet-Regí et al., 2022, SBA-15 is shown having a structure with pores arranged in hexagonal order, with *micropores* in the walls which are connecting the mesopores. Then SBA-15 is a *micro-mesopore silica material* (Ojeda-López et al., 2021).

For SBA-15 we can find a detailed description of the processes leading from the initial mixture to the mesoporous final material (Alfredsson & Wennerström, 2015). The researchers were able to identify 12 different stages. The first stage is the hydrolysis of the source of silica into Si(OH) and alcohol. The last stage is the calcination of particles at 500 °C, during which the organic polymer components are removed and the silica network consolidated. For the step number 7, the researchers are mentioning the transformation of particles containing cylindrical micelles into particles possessing an internal liquid crystalline order with 2D hexagonal symmetry. At the end of the process, we have particles having the size of 1 micron. Therefore, Alfredsson and Wennerström were able to identify the presence of a liquid crystalline internal order during one of the stages of the process.

Let us consider again the "cooperative self-assembly" process as illustrated by Wan and Zhao, sketched in

the present discuss in the Figure 2, and compare it with the sequence given by Alfredsson and Wennerström. The components for the synthesis of SBA-15 are Pluronic surfactant, silica precursor TMOS and HCl. As previously told, during the first step, the tetramethyl orthosilicate is hydrolyzed under strong acidic condition. And here it starts a sequence of polymerization reactions. Without the Pluronic block copolymer, we observe the silica polymerization which produces a silica gel. According to Alfredsson and Wennerström, the Pluronic block copolymer does not have a relevant effect on the silica polymerization but it is strongly influencing the silica networking. The Figure 2 of the paper by Alfredsson and Wennerström is giving schematically the evolution of system. We can see that the spherical micelles turn gradually into elongated cylindrical micelles, so that these micelles are able to display a liquid crystalline order (see also the work by Linton et al., 2009).

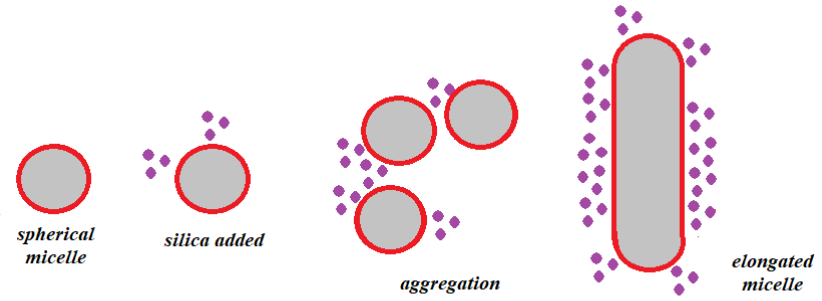

Figure 7 - A cartoon, partially according to that proposed by Alfredsson and Wennerström. From left to right: a spherical micelle, a spherical micelle surrounded by SiO_4, aggregation of micelles, elongated micelle surrounded by silicates.

In the Fig.7, the cartoon is different from that given by Alfredsson and Wennerström. The difference is in the distribution of silicates. Here we considered Emma Johansson, 2010, saying that silicate "preferably adsorbs onto low curvature sections of the micelles".

Summarizing this section, we can tell that among MSMs we can find the SBA (Santa Barbara Amorphous) materials, the FDU (Fudan University) materials, besides the Korea Advanced Institute of Science and Technology (KIT) and the MCM (Mobil Composition of Matter) materials. We have also the anionic-surfactant-templated mesoporous silica (AMS) family (Yokoi et al., 2003), and MSU-V, MSU-G and MSU-X too, which are materials referring to the mesoporous silica from Michigan State University. The article by Wan and Zhao provided detailed tables and references about MSMs, however the list is of 2007 and therefore not mentioning latest materials.

It was for sure the wide range of applications in catalysis, adsorption, and separation, that have boosted the production of so many ordered MSMs (Kim et al., 2015). In this framework we must consider that a finite number of geometries, that is of symmetry groups, exist but the different methods of preparing the mesoporous silica give different final materials, besides any further doping of them of course. In any case, the “beauty” of the templating mechanisms is coming from the already existing knowledge of LLCs (Bruckner et al., 2021).

14. Particles and supramolecular assemblies

Before discussing LLC mesophases, let us consider some further information about MSM particles and films. MCM-41 silica particles can be synthesized with several morphologies (Cai et al., 2001). In the given reference we can find nano-spherical MCM-41 silica, submicrometer-sized silica rod, and micrometer-sized oblate silica. About MCM-48, Kong et al., 2005, tell that the synthesis of single crystals is difficult. Only a few reports of MCM-48 with crystal shapes have been presented (crystals

with truncated rhombic dodecahedral shape), besides the cube morphology displayed by their publication (Kong et al., 2005). Single crystal cubes have a size of 1 micron.

About the particle size, we can find an article mentioning a *facile* synthesis route (Kim et al., 2010) to have monodisperse spherical MCM-48 MSM particles, possessing the cubic *Ia3d* symmetry of pores inside. The phase domain is extended by controlling the stirring rate and molar ratios of silica source and surfactant. Triblock-copolymer Pluronic F127 is used to determine the particle size. Kim et al. were able to control the average size of spherical MSM particles, within the range of 70−500 nm, changing the amount of F127. The researchers investigated binary systems with different non-ionic surfactants, used as "particle grain-tailors" inhibiting the grain growth. Kim et al. evidenced that the spherical particles resulting from the addition of F127 do not show aggregation between particles.

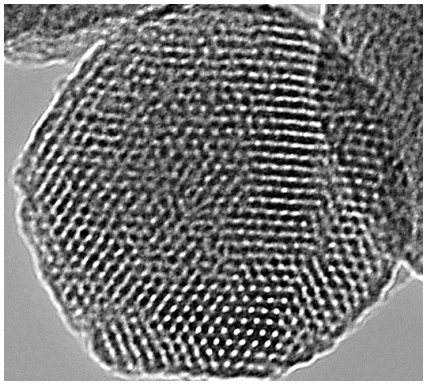

Figure 8 - TEM image of a mesoporous silica nanoparticle (Courtesy Victor Lin group at Iowa State University, has been released in the public domain, Archived). See for instance Vivero-Escoto et al., 2010, Slowing et al., 2010.

As we mentioned earlier, Kong et al., 2005, give their route to the MCM-48 monocrystals. In the article it is also specifically told that mesoporous silica particles are produced by means of a "supramolecular templating method". The authors are stressing that the material has no true crystalline order. The wall of the pores is made by amorphous silica, with a short-range order indeed, whereas the channel structure possesses a long-range order on the mesoscopic scale. About the supramolecular order, let us remember that the remarkable feature of LLCs, turning them different from TLCs, is the self-assembling of the amphiphilic molecules as supramolecular structures. These structures are the basic unit of the mesophases (Neto & Salinas, 2005). In any case, in (Kong et al., 2005), it is not mentioned LCT or TLCT but a *supramolecular templating method*.

The supramolecular template is discussed in (Beck et al. 1994; 1995). In these publications authors remember the previous works by (Kresge et al., 1992; Beck et al., 1992), and stress that the proposed mechanism for the formation of M41S (liquid crystal templating, LCT) is a method in which *supramolecular assemblies* of a surfactant serve as one component of the operative template for the formation of these materials.

According to the authors (Beck et al., 1994), the results given in the article are reinforcing the hypothesis that M41S materials are formed through a mechanism in which aggregates of cationic surfactant molecules in combination with anionic silicate species form a supramolecular structure.

In Martin et al., 2002, we can also find the templating method defined in a different manner, and the silica told as “micelle templated silica" (MTS). Martin et al. are stressing that the development of MTS has been "one of the most original fields of materials research since the seminal papers from the Kresge and Beck groups on MCM-41 and MCM-48”. It is also remarked the importance of the control of size and shape of adsorbent particles as an essential condition for any chromatographic application. The reasons to have in experimental studies, where colloidal suspensions are used, a phase consisting of homogeneous particles possessing uniform shape and size had been clearly explained by Stöber and coworkers in 1968. A monodispersed particulate suspension offers experimental and theoretical advantages. It facilitates easy calibration procedures for analytical equipment, reducing the data. A consequent easier evaluation and interpretation of experiments is possible, since the results are no longer biased by parameters concerning the size and shape particle distribution.

As previously told, Stöber et al., 1968, developed a system of chemical reactions to control the growth of spherical silica particles of uniform size. Today the method proposed in 1968 is named “Stöber method”; any method to have spherical mesoporous silica particles can be mentioned as a “modified Stöber method”.

Let us add an observation from the review by Ariga et al., 2012. About the device innovations, the researchers observed that, so far, it was due to the development of *top-down* approaches to specific microfabrication techniques. But, "those *top-down* techniques are not useful" in the case that "chemical processes are used as the operating principle". Therefore, we are forced to *bottom-up* approaches which can create novel functional materials possessing features at nanometric scale. The reason is that the bottom-up methods are based on self-assembly processes, which can produce selected structures, "through spontaneous association of atoms, molecules, clusters, and particles".

15. Hollow spheres

Let us consider here another peculiar “modified Stöber method”. In Zhu et al., 2005, we can find the preparation of hollow mesoporous silica spheres (HMSs), with a uniform size and morphology. The used co-template materials are poly-vinyl-pyrrolidone (PVP) and cetyl-trimethyl-ammonium bromide (CTAB). The hollow structure is characterized by hexagonally ordered pore channels on the shell. The researchers described the process as a typical synthesis procedure. Poly-vinyl-pyrrolidone and NaOH were dissolved into water with stirring. When the solution turns clear, CTAB was added. After its complete dissolution, TEOS is poured into the PVP/CTAB solution, vigorously stirring it for 24 h. The solution was then sealed in Teflon-lined autoclaves at 80 °C for 48 h. The product was filtrated and dried and then calcinated to remove the templates. Low-angle XRD analysis shows that calcined HMSs possesses "hexagonal symmetry structure (*P6mm*) typical for MCM-41".

As noted by Zhu et al., without the co-template PVP, the conventional MCM-41 can form at room temperature. Therefore, the role of PVP is considered as crucial to form the hollow mesoporous silica spheres. Previous literature (Tsitsilianis et al., 2000, Thibaut et al., 2000) had shown that using a given amount of PVP in a basic aqueous solution, the formation of spherical aggregates is observed. The hydrophilic parts of PVP are at the outer interface with solvent. CTAB molecules are adsorbed around the PVP aggregates. Then, the hydrolysed TEOS is assembling itself with CTAB around PVP aggregates. In this manner, the ordered MCM-41-like structure is forming the outer shell. After calcination, PVP and CTAB are removed, and the silica shell remains.

16. Dendritic mesoporous nanoparticles

We have seen the spheres with ordered mesoporous structures and the shells with MCM-41 arrangement of pores. However, other different structures exist; they are mentioned as "dendritic mesoporous silica nanoparticles" (DMSNs). As told by Xu et al., 2022, understanding the possible “dendritic structures” and their formation mechanisms is fundamentally important for applications. By means of electron tomography, two types of tree-branch-like and flower-like structures have been determined. DMSNs have central radial pore structures, that is, unconventional open pore structures in particles of uniform size. As stressed by the researchers, the DMSNs have unique properties: the pore entrance is larger than the mean pore size, the pore size distribution can be broad, the particles have generally a uniform size of the spherical morphology, and the wall structures of the pores is different from that of MSNs. Therefore, "Those structure features indicate different formation mechanisms for the “dendritic” MSNs from traditional ones" (Xu et al., 2022).

In the review by Xu et al., it is told that we can find more than 800 papers in the Web of Science indexed by keywords “dendritic mesoporous silica”, “fibrous mesoporous silica”, “radial mesoporous silica”, and that there is an "ongoing debate" concerning the formation mechanisms. This is reflected by the several terminologies that we find in literature (“dendritic”, “dendrimer-like”, “fibrous”, “wrinkle”, “radial”, “fractal”, “chrysanthemum-like”, “dandelion-type”, “stellate” and “core-cone shaped”, see the references given by Xu et al., 2022). The

formation mechanisms based on soft-template methods are discussed in the review. For example, the flower-like DMSNs have been fabricated using soft-templating in a sol–gel process. The predominant template materials are cetyl-trimethyl-ammonium bromide (CTAB), cetyl-trimethyl-ammonium chloride (CTAC), and cetyl-pyridinium bromide (CPB). "The addition of oil or specific anions along with the cationic surfactant templates is the key to the formation of the nanoparticles with flower-like morphology". More details in Xu et al., 2022.

17. **Templates for photonic crystals**

A peculiar form of surfactant-assisted templating is that producing photonic crystals. These crystals are metamaterials characterized by a periodic dielectric function, able to produce photonic bandgaps, so that electromagnetic waves cannot propagate in a specific wavelength range, known as the "gap" (Yablonovitch, 1987). The photonic bandgap (PBG) is determined by the refractive index of the dielectric medium and by the lattice parameters of photonic crystals. In (Li et al., 2020), we can find a surfactant-templated mesoporous material used to create a photonic crystal with MCM-41 geometry. In the article it is observed that the PBG of the templated material, a vertically aligned mesoporous MCM-41 film, is in the extreme ultraviolet wavelength range (5 ~ 40 nm). The film was prepared by means of an electrochemically assisted self-assembly (EASA) method on an ITO plate. The solution was made by water, ethanol, $NaNO_3$ and CTAB as surfactant. Then, TEOS was added to this mixture. After the growth of the surfactant-templated mesoporous material, the film was dried and aged, and the surfactant template removed. EASA method was proposed by Goux et al., 2009. By means of it, we can obtain highly ordered and vertically oriented mesoporous silica films.

18. Macro-mesoporous silica

When discussing the soft templating, we have mentioned the article by Wu et al., 2020. The article is deeply investigating the hierarchically structured porous materials, characterized by an interconnected hierarchical porosity. Wu et al. are reporting the recent progresses to have materials best suited for energy storage. Therefore, besides the pure MSMs, we can find a wide variety of silica materials possessing for instance macro- and mesopores.

In Roucher et al., 2019, we can find a method to produce a meso-macro-silica material. The authors consider that MSMs are produced in fine powders but some monolithic silica materials can be interesting for several applications too; therefore they are proposing to combine the emulsion templating mechanism for monolithic Si(HIPE) materials (Carn et al., 2004) with the "cooperative templating mechanism" used for the mesostructured silica. Si(HIPE)s are produced with concentrated emulsions of a system made of TTAB, dodecane, water and TEOS. Then, to the emulsion, P123 is used to control the porosity. The researchers stress that ionic and non-ionic surfactants can interact producing features different from that ascribed to the individual surfactant. For this reason, the TTAB/P123/water system has been investigated and the role of the dodecane determined, to have more information about the formation mechanism of the desired *hierarchical porous* silica, that is with macro- and meso-pores. The Figure 9 in Roucher et al., 2019, gives the appearance of the synthesized macro-mesoporous silica, besides the pore size distributions as a function of P123/TTAB ratio. As in the previous work by Roucher et al., 2018, the proposed material is a new macro-mesocellular silica SBA-15-Si(HIPE) monolith. As told before, SBA-15 is a structure with mesopores arranged in hexagonal order and micropores in the walls which are connecting the mesopores. Then, the SBA-15-Si(HIPE) monolith is a micro-meso-macroporous silica material.

What does HIPE mean? It means High Internal Phase Emulsion. As told by Depardieu et al., 2016, HIPEs are emulsions which have the total volume fraction of the droplet phase (internal phase volume fraction) exceeding 0.74. This value is coming from the most compact packing of spherical, uniform and undistorted droplets in a unit cube. Depardieu and coworkers provide a detailed description of emulsions, oil/water for instance, and their interfaces "employed as chemical reactors at a glance" (for emulsions, see please also Sharma and Shah, 1985). To enhance the thermodynamic stability of

interfaces, surfactants are used. According to the Bancroft rule (1913), a surfactant possessing higher affinity with respect to one of the phases promotes this phase to be the continuous one.

As told by Depardieu and coworkers, the interfaces in the emulsion possess a high charge density which is favoring nucleation and growth processes. In their article, the authors continue with the discussion of chemical or physical foaming and High Internal Phase Emulsions (HIPEs). The polymerization of the emulsion continuous phase, used in a soft template process, produces solid microcellular foams. However, when combined with the lyotropic mesophases, emulsions are "powerful tools to generate hierarchical porosity", as shown also by Silverstein, 2014.

19. Lyotropic phases

How many meso-structure geometries can we observe? If the LCT is a true LCT producing mesostructured material which is the inverse of an LC mesophase, then we have a finite number of symmetry groups. This is the number of mesophases observed in LLCs. And the total number of the space groups in three dimensions, which are coming from the symmetries for translation, rotation, and reflection, is quite great being of 230 (the cubic mesophase with *Ia3d* symmetry is Q^{230}).

As previously told, for LLCs we need an amphiphilic surfactant that can form aggregates through a self-assembly process when the molecules of the amphiphilic mesogen are dispersed into a non-mesogenic solvent. In aqueous media, the driving force of aggregation is due to the features of amphiphilic molecules, characterized by hydrophilic head-groups, which create surfaces into aqueous solution, able to separate the hydrophobic chains from it. In many cases the lyotropic aggregation appears when the concentration of the amphiphile exceeds the critical micelle concentration (CMC).
For a mixture of amphiphiles and water, as told by Neto & Salinas, 2005, it was in 1913 that J. W. McBain proposed the idea of micelles as aggregates of surfactant molecules (Vincent, 2014). In 1949, Peter Debye recognized the existence of a critical micellar concentration. The research groups by Per Ekwall, Vittorio Luzzati, and P. A. Winsor performed outstanding investigations, providing basic phase diagrams such as the main features of the structure of lyotropic phases. A review by Ekwall (1975) stimulated the practical application of amphiphilic compounds in cosmetics, pharmaceutical and oil industries (Guo et al., 2010).

At low concentration, above CMC, self-assembled aggregates coexist with monomeric amphiphiles in solution. The phase is not a mesophase, being isotropic. The dispersion is generally referred to as a micellar solution. At higher concentration, they appear true LLC phases. The increased concentration of amphiphile in water forces micelles to arrange regularly in space. The simplest liquid crystalline phase that is formed by spherical micelles is the 'micellar cubic', with micelles arranged in a cubic lattice (face centered cubic, body centered cubic, hexagonally closest packed). At higher amphiphile concentrations, the spherical micelles can merge to produce cylindrical aggregates, giving a long-ranged hexagonal lattice. This is the hexagonal phase. A lamellar phase, analogous of the smectic phase of TLCs, can also be observed. This phase consists of molecules arranged in bilayers separated by water. Between the hexagonal phase and the lamellar phase often a bicontinuous cubic phase appears as intermediate phase. Further increase of the amphiphilic molecular concentration can produce the "inverse" topology lyotropic phases. Inverse topology phases are more readily formed by amphiphile molecules possessing two hydrocarbon tails, such as phospholipids.

All these supramolecular structures are due to the “hydrophobic effect”, which is driving the local self-assembly of surfactant molecules to minimize the unfavorable hydrophobic contact with water and, at the same time, maximize the hydration of the hydrophilic heads of the molecules (Perroni et al., 2015). The consequent energetic arrangement, driven by the concentration, induces the formation of periodic LLC mesophases. Perroni et al. add that the *interfacial curvatures* of the supramolecular structures depend upon temperature and pressure. The molecular structure of the molecules is also fundamental.

LLCs phases are distinguished into Type I and Type II morphologies. Type I is the "normal" morphology with interfaces curved toward the hydrophobic domains. Type II is the "inverse" morphology having the interfaces curved toward water.

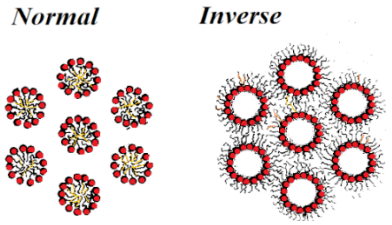

Figure 9 - Cross-section of the normal and inverse (or reverse) Hexagonal phase (heads in red, tails in grey).

For a better comprehension of LLC mesophases, let us consider the temperature-composition phase diagram of monoolein (Qiu & Caffrey, 2000; Caffrey & Cherezov, 2009), defined in the given references as the most successful lipid used for *meso-crystallogenesis*. As in Caffrey & Cherezov, 2009, let us focus on the 20 °C isotherm, starting from the cubic mesophase (see please the phase diagram at the following link https://www.ncbi.nlm.nih.gov/pmc/articles/PMC2732203/figure/F1/). This mesophase is accessed in the monoolein/water system at 20 °C, composition of about 40 % (wt/wt) water (hydration limit). The mesophase is cubic phase Q^{224} with space group *Pn3m*. In the case that some water is added beyond the hydration limit, it appears a phase corresponding to cubic phase boli sitting in an excess of precipitant solution (Caffrey & Cherezov, 2009). Moving along the 20 °C isotherm, and reducing hydration, after the cubic phase with symmetry *Pn3m*, a second cubic phase appears. It is Q^{230} phase with space group *Ia3d* (Figure 10). Continuing to reduce the water content, the lamellar liquid crystalline L_α phase is produced, a phase consisting of planar lipid bilayers, separated by water. A further reduction in water gives rise to the lamellar crystalline or L_c phase. This is not a mesophase but a true solid.

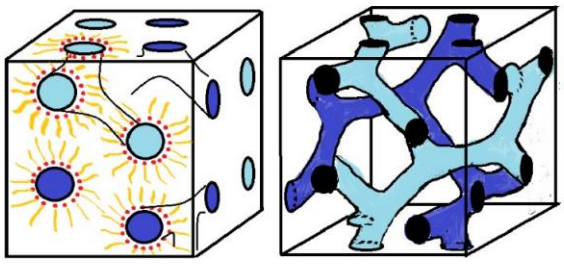

Figure 10 - Cubic structure with *Ia3d* symmetry. The model was proposed by V. Luzzati et al., 1967, 1968, as consisting of two interwoven, but not connected, networks of rods which are connected three by three. These rods represent the axes of water channels for low degrees of hydration (inverse phase). The networks are separated by a film of amphiphilic molecules. For higher degrees of hydration, the rods are the axes of cylinders of amphiphilic molecules, with the two networks separated by a film of water.

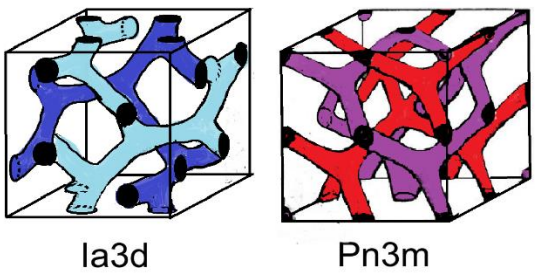

Figure 11 - *Ia3d* compared with *Pn3m*, as depicted by Tresset, 2009.

Observing the phases in the Fig.1 of Caffrey & Cherezov, 2009, available at the following link https://www.ncbi.nlm.nih.gov/pmc/articles/PMC2732203/figure/F1/, we can see that, at 20 °C, the cubic *Ia3d* is spanning a range of %w/w of water from about 23 to 37, therefore quite larger than that of the

cubic *Pn3m*. The lamellar L_α phase ranges from 10 to 20 of %w/w of water at 20 °C. At 95 °C, we can observe a hexagonal phase $H_\parallel$ from 17 to 24 of %w/w of water. In the hexagonal phase, the water is confined in cylinders the walls of which being the heads of the LLC molecules.

The phase diagram shown at the given link is redrawn from the work by Cherezov et al., 2006. Let us stress that the cubic phases observed in the given phase diagrams are inverse (reverse) cubic phases. It is clear from the cartoons accompanying the diagram. In a work that we have already mentioned, that by Mitchell et al., the phase behavior of polyoxyethylene surfactants (C_nEO_m) with water is discussed, and there we can find normal and reverse cubic phases. The researchers observed the following mesophases: normal cubic–spherical micelles (I_1), normal hexagonal (H_1), normal cubic–bicontinuous (V_1), that is Q^{230}, lamellar (L_α), reverse cubic–bicontinuous (V_2). The normal hexagonal and cubic mesophases were the templates used by Attard et al. to prepare their mesoporous silica.

To have a further illustration of the normal and reverse phases, let us use the Figure 2 of the article by Huang and Gui (2018). The article is released according to CC BY-NC 4.0. Many thanks to the authors for the precious illustration, that we arranged to obtain the following schematic view of some lyotropic mesophases (normal and reverse).

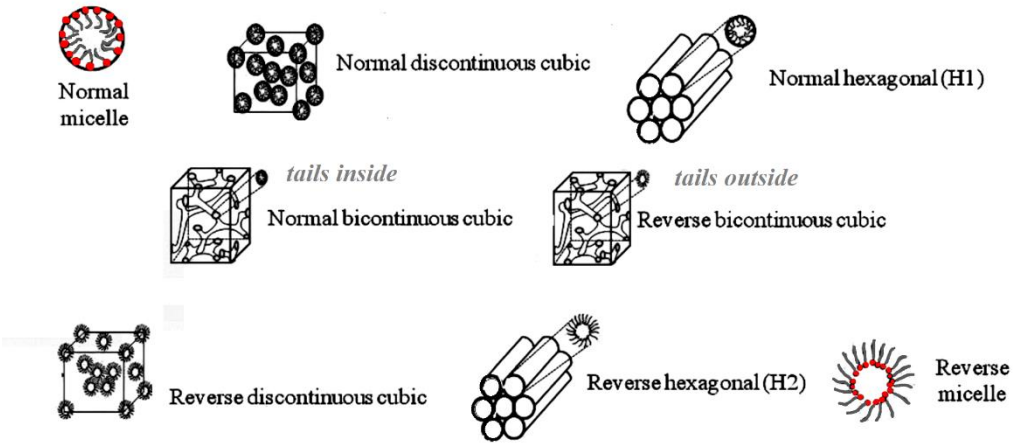

Figure 12 - Some normal and reverse phases, as illustrated by Huang and Gui (2018), in an article released according to CC BY-NC 4.0. Many thanks to the authors.

20. Cubic soft crystals

For what concerns the lyotropic cubic phase, let us stress what was told by P. Pieranski, 2011, about the soft crystals. We can find that the denomination "soft crystals" has been coined by Nozières et al., 2001, who had the purpose to mark out a special class of liquid crystalline mesophases, that is, the thermotropic and lyotropic cubic mesophases. Pieranski tells that the cubic structure is crystalline, but at the same time, it is also liquid. The huge unit cells are partially liquid (see the Figure 10). Because of their "liquid crystalline" structures, these cubic mesophases have special physical properties such as the "soft elasticity", that is, they are "soft crystals". However, it is better to add what J. Charvolin told in 1981, when considering a typical phase diagram for a potassium soap-water system. The cubic phase (*Ia3d*) has a 3-dimensional order. However, this long-range order does not result from the propagation of a short-range order at the molecular level as in crystals. Charvolin adds that this fact requires a better description of the paraffinic medium. Studies by NMR show that the disorder of the chain is dynamic. Chains are distorted by rapid isomeric rotation around their C-C bonds and the accessible conformations are limited by the anisotropic field of the interface. They diffuse in the structure with a diffusion coefficient comparable to that of liquid

paraffin. Charvolin explains that the paraffinic medium in the phase with disordered paraffinic chains may be considered as a melted paraffin constrained by the soap-water interface. Therefore, the phase can be represented pictorially as an entanglement of two liquids water and paraffin. We can consider the phase as a liquid crystalline phase in the sense that it is mixing short-range liquid state and long-range ordered state. For this reason, the lyotropic LC cubic phase is different from a classical phase of a thermotropic LC where molecules are organized in an intermediate order between crystalline and liquid states, and where short- and long-range order are directly connected.

In Neto & Salinas, 2005, we can find that the *Ia3d* space group has been the first observed example of a bicontinuous lipid/water structure (Luzzati & Spegt, 1967). It is found in a large variety of systems: hydrous soaps of divalent cations, soap, and detergent/water in the intermediate region between the lamellar and hexagonal phase, in lipid/water mixtures at low hydration and high temperature (Luzzati et al, 1968). Being so available, we can find it easily made in the MSMs.

Besides Q^{230} we can observe other cubic phases in LLCs. In 1988, Mariani et al. mentioned six cubic phases at the time identified in lipid-containing systems. According to the researchers, the structure of three of them (Q^{230}, Q^{224}, Q^{229}) can be described in terms of two three-dimensional networks of connected rods, mutually intertwined and unconnected (in the Figure 10 we have shown Q^{230}). In Q^{230}, rods are joined 3 by 3. In Q^{224} the rods are tetrahedrally joined 4 by 4 (Figure 11). In Q^{229} the rods are cubically joined 6 by 6. For the other three cubic phases, the structures of Q^{212} and Q^{227} are related to Q^{230} and Q^{224} structures respectively: one of the two networks of rods is preserved, the other network is replaced by a lattice of closed micelles. According to Mariani et al., in the case of Q^{223}, the structure seems consisting of a cage-like continuous three-dimensional network of connected globules, enclosing a three-dimensional lattice of closed micelles.

In Mariani et al., 1988, it is told that the structures of Q^{230}, Q^{224}, Q^{229} relate to three fundamental cubic infinite periodic minimal surfaces. “More interestingly, the structures of, on the one hand Q^{230}, Q^{224}, Q^{229} and of Q^{212}, Q^{227}, Q^{223} on the other, are shown to provide topological generalizations of the two paradigms of lipid organization; namely, the bilayer and the monolayer”.

The Q^{230}, Q^{224}, Q^{229} phases are the bicontinuous cubic phases. In Neto & Salinas, 2005, it is told that the structure of the bicontinuous cubic phases can be discussed from two different points of view. It can be considered either a structure of folded surfaces or a network of rod-like aggregates. This last one is the view used in the Figure 10 and 11. The cubic bicontinuous structures identified in LLCs are those of the space groups *Ia3d* (Q^{230}), *Im3m* (Q^{229}) and *Pn3m* (Q^{224}). Q^{230} phase has been observed *with both direct and inverted topology*. Q^{230} bicontinuous surface is also called “gyroid infinite periodic minimal surface” G-IPMS. This surface is in general known as a periodic minimal surface, free from self-interactions, and characterized by a mean curvature that vanish at each point of the surface (Neto & Salinas, 2005).

The space groups of Q^{212}, Q^{227}, Q^{223} are $P4_332$, *Fd3m*, *Pm3n* respectively.

21. Inverse cubic phases and membrane curvature

Shearman et al., 2006, are discussing the inverse (reverse) lyotropic phases, which are those possessing a "negative" interfacial curvature. In particular, the inverse bicontinuous cubic phases are investigated. Shearman and coworkers describe the curvature elasticity and the related packing frustration involved in the stability of inverse phases. The article of 2006 is based on the previous works of the research group on the LLC phases. According to the authors, the "most common and best characterized" of the mesophases are the bicontinuous cubic *Ia3d*, *Pn3m* and *Im3m* inverse phases, such as the hexagonal H_{II} inverse phase and the micellar cubic *Fd3m* inverse phase. The schematic view of these phases is given in the Figure 1 of their review; in the article, the inverse bicontinuous cubic phases are indicated as Q_{II}. Non-

cubic phases possessing rhombohedral or tetragonal symmetry have also, but rarely, been observed. Shearman and coworkers stress that in the commonly observed cubic phases - *Ia3d*, *Im3m* and *Pn3m* - the water channels are created in a continuous bilayer that divides the volume "into two inter-linked but separate aqueous sub-volumes".

After introducing the biological membranes as based on the self-assembly properties of amphiphilic lipids in an aqueous solution, Shearman and coworkers consider the curvature of the membranes starting from a flat lipid monolayer. The shape of the monolayer is changed when thermodynamic parameters are varied. An increase of temperature, for instance, forces the splay of the lipid molecule tails, producing a curved surface. For what concerns the curvature, at any point of the surface, a normal vector can be defined and the "principal curvatures" c_1, c_2 determined. They are the maximum and minimum values of the curvature, given as the eigenvalues of the Weingarten operator. The principal curvatures define the mean H and the Gaussian K curvatures:

$$H = \frac{1}{2}(c_1 + c_2), K = c_1 c_2$$

Peculiar surfaces are those having a saddle layout, with zero mean curvature everywhere; they are known as "minimal surfaces". These surfaces have a Gaussian curvature which is continuously varying, being non-positive everywhere. Shearman et al. tell that these mathematical surfaces were proposed by Scriven in 1976, for the description of the physical interfaces in ternary microemulsion mixtures of oil, surfactant, and water. As we have previously told, they appear in LLCs thanks to the work by Luzzati and coworkers.

In the Figure 4 of the review by Shearman et al., in the case of the inverse cubic phases *Ia3d*, *Im3m* and *Pn3m*, the bilayer mid-plane is represented by the minimal surfaces named Gyroid, Principal and Diamond (we will discuss them further on), so the cubic mesophases are named in the review as $Q_{II}^G, Q_{II}^P, Q_{II}^D$, instead of the names that we have used before. The review stresses that, although these minimal surfaces possess the same area per unit cell, the space is filled with different compactness.

In the review, the lipid packing parameter S is introduced, $S = V/al$, where V is the hydrophobic tail volume, a is the cross-sectional area of the head hydrophilic group, and l is the length hydrophobic chain in the molten state. A lipid with $1/3 < S < 1/2$ tends to form "positively curved" micellar aggregates, that is, it tends to form LLC mesophases of the "normal" Type I. In the review the authors consider the Type II, that is "inverse" mesophases, formed by lipids with parameter $S > 1$. This happens in the case of double-tail molecules, where the tail-region splays out with respect to the head region.

Regarding the total free energy of the system, which is consisting of lipid and water molecules, Shaerman et al. are mentioning the work by Kirk et al. who assumed that the free energy is based on main contributions coming from the membrane curvature, the packing of the hydrocarbon tails and the hydration and electrostatic contributions. In Kirk et al., we can find a model where the lipid free energy is ruled by four terms, that can be subdivided in two sets. The first set is given by the local averaged properties of the lipid-water interface. In each phase, these properties consist of the area per polar group, the mean curvature of the interface, the disorder of the hydrocarbon tails and hydration of polar heads. This contribution to the free energy is calculated as if the membrane were isolated. The second set of free energies includes electrostatic terms depending on the boundary at the lipid-water interface, the hydration effects relevant in short water spaces, and packing conditions of the tails.

The model of the physical interface of lipid and water is distinguishing three regions: I) the water region, which is subjected to the perturbation due to the presence of the polar groups; II) the polar group region, where we find the interaction with itself and with the water; III) the hydrocarbon region, which is preserving the interface because of its hydrophobic effect but can also exert a pressure on it, due to the fluctuations of the tails.

Shearman et al. are reporting a refinement of the model, including the hydration and electrostatic forces in the last term of the following expression:

$$g_{tot} = g_C + g_P + g_{inter}$$

g_C, g_P are the contributions coming from curvature and packing. The curvature elasticity was studied by Helfrich (1973), who modeled the lipid bilayer by means of a thin elastic surface. The deformation of this surface is associated to an energy which is depending on the curvatures of the surface, mean and Gaussian curvatures. Bending modulus, κ, and Gaussian modulus, κ_G, are introduced. The curvature elastic energy per unit area for a membrane is:

$$g_C = 2\kappa(H - H_o) + \kappa_G K$$

where H_o is the spontaneous mean curvature. The review continues with a discussion about the forces acting at the headgroup region, and those present at the polar–apolar interface and the tail–tail interactions. At the interfacial region, the system is controlled by the interfacial tension, resulting in the effect of packing the amphiphile molecules into a monolayer. About the curvature elastic parameters, the review points out that they are depending on temperature and pressure. Increasing the temperature produces an increase of the splay of the tails, consequently increasing the spontaneous mean curvature. Increasing the pressure has the opposite effect. These effects are reflected in the phase diagrams of mesophases.

The Helfrich theory implies that the bicontinuous cubic phases should be energetically degenerate, in the case that the underlying minimal surfaces have the same area. As a consequence, the three bicontinuous cubic phases mentioned above could coexist, but other interactions break the degeneracy of the cubic phases. Accordingly, Shearman et al. are reporting the experimental phase diagram of the 2:1 lauric acid / dilauroyl-phosphatidyl-choline system where the bicontinuous cubic phases are appearing with increasing hydration in the order G (*Ia3d*, Q^{230}) → D (*Pn3m*, Q^{224}) → P (*Im3m*, Q^{229}). This sequence is mentioned to be universal, but not all three cubic phases are necessarily occurring in each lyotropic system.

In Zeng et al., 2019, the above-mentioned phases are defined as double gyroid, double diamond and double primitive, which is also known as the "body-centered plumber′s nightmare". As shown in the Figure 11 for *Ia3d* and *Pn3m*, these "double" phases are rendered with double-network structures. In Zeng et al., 2019, it is stressed that, besides the double-network structures mentioned above, there are also structures created by only one network: the single gyroid, $I4_132$, Q^{214}; the single diamond, *Fd3m*, Q^{227}, and the single primitive, *Pm3m*, Q^{221}, as shown in the Figure 1 d–f of the given reference. We have encountered one of them, the Q^{227}, *Fd3m*, among the six cubic phases mentioned by Mariani et al., 1988. "The latter three are extremely rare and known only as solid-state structures, whereas they are considered as metastable in soft matter".

About the nomenclature of the cubic phases, Sorenson and Mahanthappa, 2015, stress that the numerous potential applications of the soft materials possessing such structures are requiring "concise, consistent, and unambiguous" definitions. Sorenson and Mahanthappa propose to adopt a nomenclature where the description of a mesophase is given "in terms of the total number of non-intersecting domains into which three-dimensional space is partitioned". An example is given in the Figure 1 of the given reference, where we find the single gyroid, the double gyroid, the alternating gyroid and the core-shell gyroid; these structures "mathematically derive from the G [gyroid] minimal surface" and for this reason are defined as bicontinuous phases. To Sorenson and Mahanthappa, "this classification fails to capture the number of distinct, non-intersecting, and potentially chemically different domains present in each structure".

Sakya and coworkers, 1997, point out that there are two classes of cubic phases. One class is that of the bicontinuous cubic phases, space groups *Ia3d*, *Pn3m*, *Im3m*, that in the case of type II systems are consisting of a continuous bilayer of amphiphilic molecules which divides the space into two interwoven, continuous networks of water. For type I systems, water and amphiphile are reversed. The second type of cubic mesophase is that of the micellar cubic phases consisting of discrete micellar aggregates arranged on cubic lattices. There is the *Fd3m* cubic phase and the *Pm3n* cubic phase.

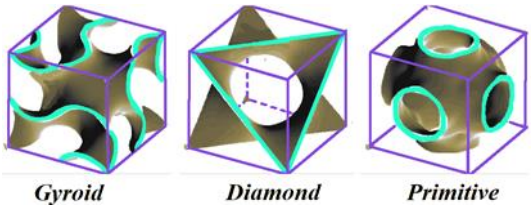

Figure 13 - For this illustration, we used the view of the surfaces given in the Figure 1 of the article by Yaghmur et al., 2007 (many thanks to the authors). The P-, D- and G-surfaces are linked by a Bonnet transformation (Lidin, 1990),

22. Why a gyroid?

Gòżdż & Hołyst, 1996, considered the surfactant molecules arranged to form minimal surfaces. The two researchers start their discussion from the ability of surfactants to solubilize oil in water, an ability which stems from the polar and nonpolar segments at two ends of the amphiphilic molecules. In this manner, surfactant molecules prefer to stay at the oil-water interface, forming monolayers. At high concentration of surfactant molecules, the interface is forming periodic structures of various symmetries. Gòżdż and Hołyst mention Luzzati et al. (1967-68) in relation to the gyroid. NMR, SAXS (small angle x-ray scattering) and surfactant concentration measurements told that the surface is like a triply periodic minimal surface, and then it has a null mean curvature at every point.

Since the discovery of minimal periodic surfaces in 1865 by Schwarz, only one periodic embedded gyroid surface of cubic symmetry and genus 5 (per unit cell) has been discovered and characterized by Schoen, 1970. Gòżdż & Hołyst define it as the Schoen-Luzzati gyroid. Intuitively, the genus is the number of "holes" of a surface (Popescu-Pampu, 2016). To explain how gyroids appear, Gòżdż and Hołyst, 1996, used an approach based on the Ginzburg-Landau model, as proposed by Teubner & Strey, 1987, in the case of a system made by oil, water and surfactant.

The phenomenological Landau free energy is given according to an expansion in the order parameter:

$$F = \int f(\phi, \nabla\phi, \Delta\phi) d^3r \qquad (1)$$

$$f = a_0 + a_1\phi + a_2\phi^2 + a_3\phi^3 + a_4\phi^4 + a_5\phi^5 + a_6\phi^6 + \cdots + c_1(\nabla\phi)^2 + c_2(\delta\phi)^2 + \cdots \quad (2)$$

Teubner and Strey discuss the truncation of the above expansion, which is depending on the considered problem. The Landau-Ginzburg free energy functional assumed by Gòżdż and Hołyst has the following form:

$$F[\phi] = \int d^3r[|\Delta\phi|^2 + g(\phi)|\nabla\phi|^2 + (\phi^2 - 1)^2(\phi^2 + f_0)] \qquad (3)$$

Here, $g(\phi) = q_2\phi^2 - g_0$; $\phi(r)$ is the order parameter representing the difference between oil and water concentration. g_2, g_0 are positive constants and f_0 is a constant (positive or negative). The last term is the bulk free energy and describes the relative stability of pure water phase, $\phi = -1$, pure oil phase $\phi = 1$, and microemulsion $\phi = 0$. When $g_2 > 2$ the system can undergo a transition to periodically ordered phases. Details are given in a further discussion proposed by Góźdź & Hołyst in the Physical Review E.

The following argument is given to understand why we must expect a minimal surface. The mean curvature is defined by:

$$H = -\frac{1}{2}\mathrm{div}\left(\frac{\nabla\phi}{|\nabla\phi|}\right) = -\frac{1}{2}\frac{\Delta\phi}{|\nabla\phi|} + \frac{1}{2|\nabla\phi|}[\nabla_n|\nabla\phi|] \qquad (4)$$

∇_n represents the derivative along the normal to the surface. The second contribution to the free energy, $\int d^3r[g(\phi)|\nabla\phi|^2]$, with $g(\phi) = q_2\phi^2 - g_0$, is minimized when, for $\phi(r) = 0$, $|\nabla\phi|$ has the maximal value. At the maximum of $|\nabla\phi|$, the normal derivative vanishes and the same happens for the second term in Eq.4. Having (3) the symmetry $\phi, -\phi$, the mean curvature H, averaged on the whole surface should be zero (Gòżdż & Hołyst, 1996). It means that either $\Delta\phi$ is exactly zero at the surface or it changes sign. Looking at the first term of Eq.3, it follows that the former case can be favored, and consequently $H = 0$ at every point at the surface. Hence, we can expect that some of the surfaces are minimal.

To find the minima of the functional, Gòżdż & Hołyst, 1996, discretized Eq.3 on the cubic lattice. Therefore, the researchers investigated the free energy with a numerical calculation, checking Ginzburg-Landau Eq.3 free energy of 30 different structures of various symmetries. They found that the only stable ordered structure is the lamellar phase.

The gyroid phase of genus 5 (Schoen-Luzzati gyroid) has the second lowest energy (after lamellar phase). In Eq.3 it follows that at $\phi(r) = 0$ the gradient term gives large and negative contribution to the energy. Gòżdż and Hołyst made some calculations for a new function $g(\phi)$ given by $g(\phi) = q_2\phi^4 - g_0$. Increasing the power of ϕ by a factor of 2 sharpened the interface between oil and water, but at the same time reduced the size of the unit cell. "The net result is the larger relative difference in energies between the gyroid and lamellar phase."

Gòżdż and Hołyst observed that, in the case of multiparameter Landau models, they expect the stabilization of the various phases which are only metastable in the model they have proposed. Among the local minima of the free-energy functional, Gòżdż and Hołyst have found four known minimal surfaces: P, D, IWP, and G (Primitive, Diamond, Gyroid, and I-WP structures). A figure representing these surfaces is given by AlMahri et al., 2021.

Then, we could consider adding parameters regarding the presence of silica in the mixture, to enhance the stability of the cubic "gyroid" phase, and explain the observed phases also without a TLCT mechanism.
About the minimal surfaces in general, we can consider the variational problem for the area functional $A[f] = \int \sqrt{1 + |\nabla f|^2}\, d^n x$, where we have the gradient ∇f in an *n*-dimensional space. Constrained to a given contour $f = \zeta$ on ∂U the boundary of domain *U*, any critical f must be:

$$0 = \left[\frac{d}{d\epsilon} A[f + \epsilon\eta]\right]_{\epsilon=0}$$
$$= \int \frac{\nabla f \cdot \nabla \eta}{\sqrt{1 + |\nabla f|^2}}\, dx$$
$$= -\int \eta \,\mathrm{div}\left(\frac{\nabla f}{\sqrt{1+|\nabla f|^2}}\right) dx.$$

Being the mean curvature also defined as $H = \mathrm{div}\frac{\nabla f}{\sqrt{1+|\nabla f|^2}}$, this curvature is zero for minimal surfaces. In 2-dimensions:

$$H = \frac{Lf}{\left(\sqrt{1+|\nabla f|^2}\right)^3},$$
$$L = (1 + f_x^2)\partial_{yy} - 2f_x f_y \partial_{xy} + (1 + f_y^2)\partial_{xx}.$$

Then, $Lf = 0$, which is the Lagrange equation, 1760.

Classical examples of minimal surfaces are the plane, found by Lagrange, the catenoids, surfaces made by rotating a catenary, and the helicoids, that is surfaces obtained by a line rotating around an axis perpendicular to the line. Then we have the surfaces found in the 19th century: Schwarz minimal surfaces, which are periodic surfaces that fill R^3, Riemann's minimal surface, Enneper surface, Henneberg surface and others. The modern surfaces include the Gyroid, which is one of the Schoen's surfaces from 1970. As previously told, it is also known as a TPMS (triply periodic minimal surface), that is periodic in three independent directions. Being free of self-intersections it is said to be embedded.

Quite useful are the representations. Among them, the Enneper–Weierstrass representation gives the coordinates of the Gyroid as (Gandy and Klinowski, 2000):

$$x = \mathrm{Re}\int_{\omega_0}^{\omega} e^{i\theta_G} F(\tau)(1 - \tau^2) d\tau \;;$$
$$y = \mathrm{Re}\int_{\omega_0}^{\omega} ie^{i\theta_G} F(\tau)(1 + \tau^2) d\tau \;;$$
$$z = \mathrm{Re}\int_{\omega_0}^{\omega} 2e^{i\theta_G} \tau F(\tau) d\tau$$

with Weierstrass function: $F(\tau) = (1 - 14\tau^4 + \tau^8)^{-1/2}$. and $\theta_G \approx 38.0147740°$.

A specific minimal surface can be determined by integrating its Weierstrass function. The integrals can always be evaluated by numerical integration, but so far could be calculated analytically for only a few surfaces, as told by Gandy and Klinowski, 2000. The Enneper–Weierstrass representation of the Gyroid surface involves integrals which can be evaluated analytically and are expressed in terms of the incomplete elliptic integral of the first kind (EllipticF). After a double substitution, the integrals given above are reduced to elliptic integrals. Incomplete elliptic integrals are functions of two arguments and the complete elliptic integrals are functions of a single argument. In this manner the *x* coordinate, for instance, becomes:

$$x = \kappa e^{i\theta}\mathrm{Re}\left\{\frac{1}{2\sqrt{2}} EllipticF\left[X, \frac{1}{4}\right]\right\}$$
$$\text{where: } X = \mathrm{ArcSin}\left(\frac{2\sqrt{2}\omega}{\sqrt{\omega^4+4\omega^2+1}}\right).$$

For κ, θ see please Gandy and Klinowski. 2000. As told by Gandy and Klinowski, although the properties of the TPMS follow uniquely from the Weierstrass function, this function is known only for several TPMS of simple topology. The Weierstrass function may be constructed if there exists a "surface patch" from which the whole TPMS can be generated. This is the case for the Gyroid.

The triply periodic minimal surfaces (TPMS) are infinitely extended and have one of the crystallographic space groups as symmetry group, there are no self-intersections, and they subdivide the space into two labyrinthine regions. The topology of the surface is generally depicted by two interpenetrating networks (Lord and Mackay, 2003), but a single network can also be used (Zeng et al., 2019). In fact, as noted by Lord and Mackay too, from the cubic unit cell of space group *Pn3m* we can pass to the *Fd3m* group. When the two sides of the Diamond surface are colored with different colors, the cells have alternate colors, and the space group becomes *Fd3m*. The Diamond-surface (D-surface) has a corresponding labyrinth graph with four diamond connections. Using a formula by Weierstrass, Schwarz obtained an analytic expression for the D-surface. The same was done for the Primitive-surface (P-surface), where the labyrinth is a network based on a primitive cubic lattice. As previously told, the next TPMS was obtained by Schoen who investigated for NASA the existence of surfaces suitable to be used in space structures. According to Lord and Mackay, more than a dozen new examples had been given. "Those surfaces with cubic symmetry are called (following Schoen's rather eccentric notation) IWP, FRD, OCTO, C(D) and G ('the gyroid')". Gòźdź and Hołyst have discovered two more cubic TPMS defined BFY ('the Butterfly') and CPD. Lord and Mackay stress that some minimal surfaces can be described by expressions providing the coordinates of all points of the surface, but expressions are complicated and, as we have seen before for the gyroid, involve elliptic functions.

23. Phase transitions

Let us consider once more the phase diagram in the Fig.1 of Caffrey & Cherezov, 2009, assuming a fixed composition, for instance 22 %w/w of water. In the temperature range from 40 °C to 95 °C, we can observe the phase transition from the cubic *Ia3d* phase to the hexagonal phase. This is a quite drastic rearrangement of molecules, passing from a branched structure into one formed by long parallel cylinders. The problem of transitions from and into a cubic LLC phase had been addressed by Clerc et al., 1991. In the given reference, the researchers provided results obtained in the $C_{12}EO_6$/water binary system, which exhibits the bicontinuous cubic *Ia3d* mesophase, and two transitions toward the hexagonal and lamellar mesophases. At a composition of 65 % in wt of $C_{12}EO_6$/water, we can find the following transitions driven by temperature: Hexagonal – 16 °C – Cubic – 31 °C – Lamellar. In (Clerc et al., 1991), the epitaxial relations occurring at the two transitions are mentioned. These relations were first established by Rançon and Charvolin, 1987, and they are telling that two adjacent mesophases are always strongly related: a cubic mesophase grows with a fixed orientation with respect to a hexagonal one and a lamellar mesophase develops with the lamellar planes perpendicular to direction of the cubic mesophase (Rançon & Charvolin, 1987).

Of the cubic *Ia3d* mesophase, one of the most striking features is the bicontinuity, which means that, at high degrees of hydration, only two equivalent surfactant media, separated by a water film, exist (normal phase). The bicontinuity imposes the shape of the water film (Charvolin & Sadoc, 1988). The shape is that of an infinite periodic minimal surface, which is dividing the space into two equivalent subspaces, being at the same time periodic and infinite. As previously seen, the space group *Ia3d* imposes the Schoen's Gyroid surface (Rançon & Charvolin, 1987). In (Rançon & Charvolin, 1987), it is stressed that the two subspaces are filled with two 3D-networks of connected surfactant "rods", according to Luzzati et al. description. All the rods have equal length and meet three by three at the angle of 120° at planar nodes.

Rançon and Charvolin, 1987, aimed to understand how the parallel cylinders in a hexagonal mesophase becomes connected to produce the two 3D-networks of the cubic structure. The cubic mesophase has the preference to develop along the cylinder direction.

This direction transforms into a [111] cubic direction. At the transition, the cylinders transform following two different ways. Two thirds of the cylinders become helices, each helix being entirely contained in one of the 3D-networks, with right-handed helices in one network and left-handed in the other. The last third created the connections of the two networks.

In (Mariani et al., 1994), three lipid-water systems (namely PaLPC, OLPC and DTAC), which exhibit mesophases including hexagonal and the cubic bicontinuous Q^{230} (*Ia3d*) and/or the cubic micellar Q^{223} (*Pm3n*) phases have been investigated. The epitaxial relationships occurring at the hexagonal to cubic phase transition have been also considered in the given reference, so that to analyze the growth of the hexagonal phase from the Q^{230} cubic phase and from the globular micelles packed in the Q^{223} cubic phase. By means of an approach based on the electron density distribution of the cubic phase in the direction of the cylinder growth, Mariani et al. (1994) proposed a mechanism for the process of transformation of the structural elements in the mesophases.

In (Conn et al., 2006), authors focus on a phase transition where membrane fusion occurs, from lamellar to inverse bicontinuous cubic phase transition. In fact, some models (Chernomordik & Kozlov, 2003; Kozlovsky et al., 2002; Siegel, 1986) have been previously proposed relying on the formation of transient lipid contacts, which are known as “stalks”, that is, the first step in the formation of the tubular connections in the inverse bicontinuous cubic phases. The case described in (Conn et al., 2006) is that of spherical onion vesicles consisting of concentric bilayers. The transition starts from thermal undulations in the lamellar phase, which disappear as interlamellar attachments are formed. When the tension reaches a critical value, the attachments are broken and it is forming a disordered network of funnels, through which water flows from the center of the vesicles. Then, the disordered texture soon resolves into ordered bicontinuous cubic structures (Conn et al., 2006). In 2018, further observations obtained by means of cryogenic transmissions electron microscopy have confirmed this pathway (Tran et al., 2018). About the phase transitions where lamellar, hexagonal, and cubic phase are involved, discussion is given also in Neto & Salinas, 2005.

24. From hexagonal phase to cubic phase

In Omer et al., 2009, we can find a high-resolution cryogenic-electron microscopy study of a hexagonal-to-bicontinuous cubic phase transition, observed during the synthesis of a mesosilica. The study concerns the evolution of the system with Pluronic P123 and butanol to form an *Ia3d* mesoporous material. The researchers stress that the cubic *Ia3d* structure is attractive for those applications which are susceptible to pore blockage. Moreover, the diffusion through a film with cubic symmetry has been shown more efficient than through a hexagonal film (Wei & Hillhouse, 2007). It was determined that the diffusion through the *Ia3d* phase was larger by over an order of magnitude, with respect to other cubic structures.

In the study by Omer et al., 2009, the researchers investigated the synthesis of the original KIT-6 and a modified synthesis, that is that of SBA-15 with butanol added some time after the precipitation. The synthesis is designated as SBA-15+BuOH. The researchers observed the structural evolution from the hexagonal mesophase to the cubic mesophase in the two reactions. Cryo-HRSEM and FFR-TEM images show that the hexagonal phase is modified into a perforated layer (PL) phase, which becomes the bicontinuous cubic phase. The formation mechanism is illustrated by the researchers, using cylinders in the hexagonal phase which are merging into a PL structure. The additional polymerization of silica modifies the PL structure into the stable *Ia3d* cubic phase.

25. ASM-10 with bicontinuous cubic Pn3m symmetry

As we have seen, LLCs possess the six cubic phases mentioned by Mariani et al., 1988. What of these cubic phases have been observed frozen in silica? Let us consider the article by Gao et al., 2006. Authors tell that, at the time, many well-ordered mesoporous materials have been successfully synthesized and that it has been claimed that these materials have different meso-structures such as orthorhombic, tetragonal, three-dimensional (3D) hexagonal, micellar cubic, bicontinuous cubic (*Ia3d*, *Im3m* and *Pn3m*),

rectangular, hexagonal and lamellar phase (and here we can easily find the list of lyotropic phases described by Neto & Salinas, 2005). "Most structures have been proposed on the basis of a combination of powder X-ray diffraction (XRD) studies and an *accumulated knowledge of liquid-crystalline phases*, whilst only a few have been precisely determined by electron crystallography".

Gao et al. report of ordered mesoporous structures with the *Pn3m* space group. For the preparation, it had been used anionic surfactants and co-structure-directing agents (CSDAs). The introduction of CSDAs into the reaction system is producing interactions between anionic surfactants and inorganic species and the control of the packing parameter. The MSM produced is AMS-10 (anionic surfactant templated mesoporous silica n. 10), exhibiting bicontinuous double diamond cubic *Pn3m*. But AMS-10 is not alone: the article is mentioning tetragonal *P42/mnm* cage type (AMS-9), cubic *Fd3m* cage type (AMS-8), 2D hexagonal *p6mm* cylindrical (AMS-3).

ASM anionic surfactant templated mesoporous silica systems have been considered in Miyasaka et al. who in 2012 investigated the role of curvature in MSMs, in particular the *Im3m*, *Pn3m* and *Ia3d* phases.

About cubic gyroid *Ia3d* and double diamond *Pn3m* phases, let us conclude mentioning a recent article where they been further investigated (Das et al., 2019). The reference is a study of the role of topology on the water inside these two cubic systems, with the same water content (22%). The research evidenced a difference in the hydration dynamics inside the two mesophases, where the water molecules confined in the *Ia3d* phase exhibit a slower dynamic compared to that in *Pn3m*. Researchers believe that this correlation between the structural topology of the different cubic mesophases and the water nanochannel can help in applications of the cubic phases. Actually, Das et al. research is an example of further analyses that LLC mesophases, such as LC templates, cubic phases are requiring.

For what is regarding water in MSM, let us consider that mesoporous materials are fundamental for studying the Gibbs–Thomson effect. This phenomenon is related to the shift, with respect to bulk systems, of the melting and freezing temperatures of confined fluid substances. It is observed in porous frameworks as a function of pore size. In Sparavigna, 2023, we considered the literature regarding the Gibbs-Thomson effect as observed for the confinement of water in mesoporous silica, porous carbon materials and biochar.

26. SBA-12 MSM

We have mentioned some of the mesophases of LLCs and assumed that the related space groups are also those observed in MSMs. However, there is a case which needs to be considered for its peculiarity. It is that of SBA-12 MSM. This material is displaying a mixture of the close-packed cubic phase with a small amount of the 3D hexagonal close packed phase, as given by Sakamoto, et al. (2002). Variations in percentage are observed according to the different synthesis procedures. Sakamoto et al. conclude that the intergrowth of the ordered meso-structures is tunable, and this could be interesting for hierarchical mesopore materials.

Let us stress that we can also observe mesophases intergrowth in LLCs. In the P123–EAN LLC, cubic *Fm3m* and hexagonal phases are coexisting in a region of the phase diagram (Chen et al., 2012). Both MSMs and LLCs display the coexistence of different space groups.

27. Conclusion

Here we are giving a comprehensive work about the liquid crystal templating (LCT) of mesoporous silica materials (previous discussions in Sparavigna, 2022). At the beginning, LCT was proposed as a surfactant templating method, able to produce meso-structured scaffolds having the same space group of LLCs mesophases. LCT has been questioned and TLCT introduced. If the surfactant concentration is lower than that suitable to form the liquid crystalline phases, the appearance of the ordered mesophases is ascribed to the interaction between the silicate species in the solution and the external micellar surface, in a process based on a "cooperative self-assembly mechanism", where the silicate oligomers and the surfactant species influence each other during

the polymerization leading to the growing of a liquid crystalline order.

We have seen some of the methods (LCT, TLCT and modified Stöber) to produce some MSMs, and discussed, specifically, the cubic phases. In the work by Gòżdż and Hołyst, about the use of a multiparameter Ginzburg-Landau models, we find proposed the stabilization of metastable phases by adding parameters in the model. In this framework we could consider adding parameters regarding the presence of silica in the mixture, to enhance the stability of the cubic "gyroid" phase, for instance, and explain the observed phases also without any TLCT mechanism. The templating method turns consequently into a modified Stöber process, based on cooperative mechanisms.

References

1. Aleandri, S., & Mezzenga, R. (2020). The physics of lipidic mesophase delivery systems. Physics today, 73(7), 38-45.
2. Alfredsson, V., & Wennerström, H. (2015). The dynamic association processes leading from a silica precursor to a mesoporous SBA-15 material. Accounts of Chemical Research, 48(7), 1891-1900.
3. AlMahri, S., Santiago, R., Lee, D. W., Ramos, H., Alabdouli, H., Alteneiji, M., Guan, Z., Cantwell, W. & Alves, M. (2021). Evaluation of the dynamic response of triply periodic minimal surfaces subjected to high strain-rate compression. Additive Manufacturing, 46, 102220.
4. ALOthman, Z. A. (2012). A review: fundamental aspects of silicate mesoporous materials. Materials, 5(12), 2874-2902.
5. Ariga, K., Vinu, A., Yamauchi, Y., Ji, Q., & Hill, J. P. (2012). Nanoarchitectonics for mesoporous materials. Bulletin of the Chemical Society of Japan, 85(1), 1-32.
6. Attard, G.S., Glyde, J.C., & Goltner, C.G. (1995). Liquid crystalline phases as templates for the synthesis of mesoporous silica. Nature, 378, 366–368.
7. Attard, G. S., Edgar, M., & Göltner, C. G. (1998). Inorganic nanostructures from lyotropic liquid crystal phases. Acta Materialia, 46(3), 751-758.
8. Bancroft, W. D. (1913). The theory of emulsification, V. The Journal of Physical Chemistry, 17(6), 501-519.
9. Bagshaw, S. A., Prouzet, E., & Pinnavaia, T. J. (1995). Templating of mesoporous molecular sieves by nonionic polyethylene oxide surfactants. Science, 269(5228), 1242-1244.
10. Basso, A. M., Nicola, B. P., Bernardo-Gusmao, K., & Pergher, S. B. (2020). Tunable effect of the calcination of the silanol groups of KIT-6 and SBA-15 mesoporous materials. Applied Sciences, 10(3), 970.
11. Bearat, H. H., & Vernon, B. L. (2011). Environmentally responsive injectable materials. In Injectable biomaterials (pp. 263-297). Woodhead Publishing.
12. Beck, J. S., Vartuli, J. C., Roth, W. J., Leonowicz, M. E., Kresge, C. T., Schmitt, K. D., Chu, C. T. W., Olson, D. H., Sheppard, E. W., & McCullen, S. B. (1992). A new family of mesoporous molecular sieves prepared with liquid crystal templates. J. Am. Chem. Soc. 1992, 114, 10834−10843.
13. Beck, J. S., Vartuli, J. C., Kennedy, G. J., Kresge, C. T., Roth, W. J., & Schramm, S. E. (1994). Molecular or supramolecular templating: defining the role of surfactant chemistry in the formation of microporous and mesoporous molecular sieves. Chemistry of Materials, 6(10), 1816-1821.
14. Beck, J. S., Vartuli, J. C., Kennedy, G. J., Kresge, C. T., Roth, W. J., & Schramm, S. E. (1995). Molecular or supramolecular templating: defining the role of surfactant chemistry in the formation of M41S and zeolitic molecular sieves. In Studies in Surface Science and Catalysis (Vol. 98, pp. 15-16). Elsevier.
15. Benamor, T., Vidal, L., Lebeau, B., & Marichal, C. (2012). Influence of synthesis parameters on the physico-chemical characteristics of SBA-15 type ordered mesoporous silica. Microporous and Mesoporous Materials, 153, 100-114.
16. Boissière, C., Van Der Lee, A., El Mansouri, A., Larbot, A., & Prouzet, E. (1999). A double step synthesis of mesoporous micrometric spherical MSU-X silica particles. Chemical Communications, (20), 2047-2048.
17. Boissière, C., Larbot, A., van der Lee, A., Kooyman, P. J., & Prouzet, E. (2000). A new synthesis of mesoporous MSU-X silica controlled by a two-step pathway. Chemistry of materials, 12(10), 2902-2913.
18. Bruckner, J. R., Bauhof, J., Gebhardt, J., Beurer, A. K., Traa, Y., & Giesselmann, F. (2021). Mechanisms and intermediates in the true liquid crystal templating synthesis of mesoporous silica materials. The Journal of Physical Chemistry B, 125(12), 3197-3207.
19. Caffrey, M., & Cherezov, V. (2009). Crystallizing membrane proteins using lipidic mesophases. Nature protocols, 4(5), 706-731.
20. Cai, Q., Luo, Z. S., Pang, W. Q., Fan, Y. W., Chen, X. H., & Cui, F. Z. (2001). Dilute solution routes to various controllable morphologies of MCM-41 silica with a basic medium. Chemistry of materials, 13(2), 258-263.
21. Carlton, R. J., Hunter, J. T., Miller, D. S., Abbasi, R., Mushenheim, P. C., Tan, L. N., & Abbott, N. L. (2013). Chemical and biological sensing using liquid crystals. Liquid crystals reviews, 1(1), 29-51.
22. Carn, F., Colin, A., Achard, M. F., Deleuze, H., Sellier, E., Birot, M., & Backov, R. (2004). Inorganic monoliths hierarchically textured via concentrated direct emulsion and micellar templates. Journal of Materials Chemistry, 14(9), 1370-1376.
23. Chandrasekhar, S. (1992). Liquid Crystals, Cambridge University Press, Cambridge and New York.
24. Charvolin, J. (1981). Interfaces of amphiphilic molecules and lyotropic liquid crystals. In Cristalli Liquidi, Atti della Scuola Nazionale del GNCL, UNICAL 1981.
25. Charvolin, J., & Sadoc, J. F. (1988). Films of amphiphiles: packing constraints and phase diagrams. The Journal of Physical Chemistry, 92(20), 5787-5792.
26. Chen, Z., Greaves, T. L., Fong, C., Caruso, R. A., & Drummond, C. J. (2012). Lyotropic liquid crystalline phase

behaviour in amphiphile–protic ionic liquid systems. Physical Chemistry Chemical Physics, 14(11), 3825-3836.
27. Cherezov, V., Clogston, J., Papiz, M. Z., & Caffrey, M. (2006). Room to move: crystallizing membrane proteins in swollen lipidic mesophases. Journal of molecular biology, 357(5), 1605-1618.
28. Chernomordik, L. V., & Kozlov, M. M. (2003). Protein-lipid interplay in fusion and fission of biological membranes. Annual review of biochemistry, 72(1), 175-207.
29. Chien, S. C., Pérez-Sánchez, G., Gomes, J. R., Cordeiro, M. N. D., Jorge, M., Auerbach, S. M., & Monson, P. A. (2017). Molecular simulations of the synthesis of periodic mesoporous silica phases at high surfactant concentrations. The Journal of Physical Chemistry C, 121(8), 4564-4575.
30. Chiola, V., Ritsko, J. E., & Vanderpool, C. D. (1971). Process for producing low-bulk density silica. Application No. US 3556725D A filed on 26-Feb-1969. Publication No. US 3556725 A published on 19-Jan-1971.
31. Clerc, M., Levelut, A. M., & Sadoc, J. F. (1991). Transitions between mesophases involving cubic phases in the surfactant-water systems. Epitaxial relations and their consequences in a geometrical framework. Journal de Physique II, 1(10), 1263-1276.
32. Collings, P. J., & Hird, M. (2017). Introduction to liquid crystals: chemistry and physics. CRC Press.
33. Conn, C. E., Ces, O., Mulet, X., Finet, S., Winter, R., Seddon, J. M., & Templer, R. H. (2006). Dynamics of structural transformations between lamellar and inverse bicontinuous cubic lyotropic phases. Physical review letters, 96(10), 108102.
34. Das, K., Roy, B., Satpathi, S., & Hazra, P. (2019). Impact of topology on the characteristics of water inside cubic lyotropic liquid crystalline systems. The Journal of Physical Chemistry B, 123(18), 4118-4128.
35. Debye, P. (1949). Light scattering in soap solutions. The Journal of Physical Chemistry, 53(1), 1-8.
36. Demus, D., & Richter, L. (1980). Textures of liquid crystals. Deutscher Verlag für Grundstoffindustrie.
37. Depardieu, M., Nollet, M., Schmitt, V., & Backov, R. (2016). Integrative chemistry: Positioning chemical reactors within the geometric space as a tool for the design of advanced functional materials. Comptes Rendus Chimie, 19(1-2), 216-230.
38. Dierking, I. (2003). Textures of liquid crystals. John Wiley & Sons.
39. Di Renzo, F., Cambon, H., & Dutartre, R. (1997). A 28-year-old synthesis of micelle-templated mesoporous silica. Microporous Materials, 10(4-6), 283-286.
40. Doane, J. W., Golemme, A., West, J. L., Whitehead Jr, J. B., & Wu, B. G. (1988). Polymer dispersed liquid crystals for display application. Molecular Crystals and Liquid Crystals, 165(1), 511-532.
41. Eftekhari, A., & Fan, Z. (2017). Ordered mesoporous carbon and its applications for electrochemical energy storage and conversion. Materials Chemistry Frontiers, 1(6), 1001-1027.
42. Ekwall, P. (1975). Composition, properties and structures of liquid crystalline phases in systems of amphiphilic compounds. In Advances in liquid crystals (Vol. 1, pp. 1-142). Elsevier.
43. Fang, Q. R., Makal, T. A., Young, M. D., & Zhou, H. C. (2010). Recent advances in the study of mesoporous metal-organic frameworks. Comments on Inorganic Chemistry, 31(5-6), 165-195.
44. Galarneau, A., Nader, M., Guenneau, F., Di Renzo, F., & Gedeon, A. (2007). Understanding the stability in water of mesoporous SBA-15 and MCM-41. The Journal of Physical Chemistry C, 111(23), 8268-8277.
45. Gandy, P. J., & Klinowski, J. (2000). Exact computation of the triply periodic G (Gyroid) minimal surface. Chemical Physics Letters, 321(5-6), 363-371.
46. Gao, C., Sakamoto, Y., Sakamoto, K., Terasaki, O., & Che, S. (2006). Synthesis and Characterization of Mesoporous Silica AMS-10 with Bicontinuous Cubic Pn3m Symmetry. Angewandte Chemie International Edition, 45(26), 4295-4298.
47. Gascón, V., Márquez-Alvarez, C., Díaz, I., & Blanco, R. M. (2016). Hybrid Ordered Mesoporous Materials as Supports for Permanent Enzyme Immobilization Through Non-covalent Interactions. Non-covalent Interactions in the Synthesis and Design of New Compounds, 345-360.
48. Giraldo, L. F., López, B. L., Pérez, L., Urrego, S., Sierra, L., & Mesa, M. (2007). Mesoporous silica applications. In Macromolecular symposia (Vol. 258, No. 1, pp. 129-141). Weinheim: WILEY-VCH Verlag.
49. Goux, A., Etienne, M., Aubert, E., Lecomte, C., Ghanbaja, J., & Walcarius, A. (2009). Oriented mesoporous silica films obtained by electro-assisted self-assembly (EASA). Chemistry of Materials, 21(4), 731-741.
50. Gov, N., Borukhov, I., & Goldfarb, D. (2006). Morphological transitions during the formation of templated mesoporous materials: Theoretical modeling. Langmuir, 22(2), 605-614.
51. Gòźdź, W., & Hołyst, R. (1996). From the Plateau problem to periodic minimal surfaces in lipids and diblock copolymers. Macromol. Theory Simul., 1996, 5, 321–332.
52. Gòźdź, W., & Hołyst, R. (1996). High genus periodic gyroid surfaces of nonpositive Gaussian curvature. Physical review letters, 76(15), 2726.
53. Góźdź, W. T., & Hołyst, R. (1996). Triply periodic surfaces and multiply continuous structures from the Landau model of microemulsions. Physical Review E, 54(5), 5012.
54. Grün, M., Lauer, I., & Unger, K. K. (1997). The synthesis of micrometer-and submicrometer-size spheres of ordered mesoporous oxide MCM-41. Advanced Materials, 9(3), 254-257.
55. Guo, C., Wang, J., Cao, F., Lee, R. J., & Zhai, G. (2010). Lyotropic liquid crystal systems in drug delivery. Drug discovery today, 15(23-24), 1032-1040.
56. Helfrich, W. (1973). Elastic properties of lipid bilayers—theory and possible experiments Z. Naturf., c 28, 693–703.
57. Huang, L., Wang, H., Wang, Z., Mitra, A., Zhao, D., & Yan, Y. (2002). Cuprite nanowires by electrodeposition from lyotropic reverse hexagonal liquid crystalline phase. Chemistry of materials, 14(2), 876-880.
58. Huang, C. H., Chang, K. P., Ou, H. D., Chiang, Y. C., & Wang, C. F. (2011). Adsorption of cationic dyes onto mesoporous silica. Microporous and Mesoporous Materials, 141(1-3), 102-109.
59. Huang, Y., & Gui, S. (2018). Factors affecting the structure of lyotropic liquid crystals and the correlation between structure and drug diffusion. RSC advances, 8(13), 6978-6987.

60. Huo, Q., Margolese, D.I., Ciesla, U., Demuth, D.G., Feng, P., Gier, T.E., Sieger, P., Firouzi, A., & Chmelka, B.F. (1994). Organization of organic molecules with inorganic molecular species into nanocomposite biphase arrays. Chemistry of Materials, 6(8), pp.1176-1191.
61. Iler, K. R. (1979). The chemistry of silica. Solubility, polymerization, colloid and surface properties and biochemistry of silica. Wiley.
62. Janus, R., Natkański, P., Wądrzyk, M., Lewandowski, M., Michalik, M., & Kuśtrowski, P. (2022). Surface-Selective Deposition of Poly(Furfuryl Alcohol) in Mesoporous Silica Template: A Cornerstone of Facile and Versatile Synthesis of High-Quality Cmk-Type Carbon Replicas. Nanocasting of Sba-15, Sba-16, and Kit-6. Available at SSRN: https://ssrn.com/abstract=4033373 or http://dx.doi.org/10.2139/ssrn.4033373
63. Jervis, H. B., Bruce, D. W., Raimondi, M. E., Seddon, J. M., Maschmeyer, T., & Raja, R. (1999). Templating mesoporous silicates on surfactant ruthenium complexes: a direct approach to heterogeneous catalysts. Chemical Communications, (20), 2031-2032.
64. Johansson, E. M. (2010). Controlling the Pore Size and Morphology of Mesoporous Silica. Linköping Studies in Science and Technology. Licentiate Thesis No. 1451. ISBN: 978-91-7393-305-6, ISSN: 0280-7971, LiU-tryck, Linköping, Sweden, 2010
65. Karamikamkar, S., Naguib, H. E., & Park, C. B. (2020). Advances in precursor system for silica-based aerogel production toward improved mechanical properties, customized morphology, and multifunctionality: A review. Advances in colloid and interface science, 276, 102101.
66. Kim, T. W., Kleitz, F., Paul, B., & Ryoo, R. (2005). MCM-48-like large mesoporous silicas with tailored pore structure: facile synthesis domain in a ternary triblock copolymer− butanol− water system. Journal of the American Chemical Society, 127(20), 7601-7610.
67. Kim, T. W., Chung, P. W., & Lin, V. S. Y. (2010). Facile synthesis of monodisperse spherical MCM-48 mesoporous silica nanoparticles with controlled particle size. Chemistry of Materials, 22(17), 5093-5104.
68. Kim, H. J., Yang, H. C., Chung, D. Y., Yang, I. H., Choi, Y. J., & Moon, J. K. (2015). Functionalized mesoporous silica membranes for CO2 separation applications. Journal of Chemistry, Volume 2015, Article ID 202867, https://doi.org/10.1155/2015/202867
69. Kirk, G. L., Gruner, S. M., & Stein, D. L. (1984). A thermodynamic model of the lamellar to inverse hexagonal phase-transition of lipid-membrane water-systems. Biochemistry 23, 1093–102.
70. Kleitz, F., Choi, S. H., & Ryoo, R. (2003). Cubic Ia3d large mesoporous silica: synthesis and replication to platinum nanowires, carbon nanorods and carbon nanotubes. Chemical Communications, (17), 2136-2137.
71. Kleitz, F., Liu, D., Anilkumar, G. M., Park, I. S., Solovyov, L. A., Shmakov, A. N., & Ryoo, R. (2003). Large cage face-centered-cubic Fm3m mesoporous silica: synthesis and structure. The Journal of Physical Chemistry B, 107(51), 14296-14300.
72. Kozlovsky, Y., Chernomordik, L. V., & Kozlov, M. M. (2002). Lipid intermediates in membrane fusion: formation, structure, and decay of hemifusion diaphragm. Biophysical journal, 83(5), 2634-2651.
73. Kresge, C. T., Leonowicz, M. E., Roth, W. J., Vartuli, J. C., & Beck, J. S. (1992). Ordered mesoporous molecular sieves synthesized by a liquid-crystal template mechanism. Nature, 359, 710−712.
74. Lagerwall, J. P., & Scalia, G. (2012). A new era for liquid crystal research: Applications of liquid crystals in soft matter nano-, bio-and microtechnology. Current Applied Physics, 12(6), 1387-1412.
75. Lagrange. J. L. (1760). Essai d'une nouvelle methode pour determiner les maxima et les minima des formules integrales indefinies. Miscellanea Taurinensia 2, 325(1), 1760.
76. Landau, L. D., & Lifshitz, E. M. (2013). Statistical Physics: Volume 5 (Vol. 5). Elsevier.
77. Li, Z., Barnes, J. C., Bosoy, A., Stoddart, J. F., & Zink, J. I. (2012). Mesoporous silica nanoparticles in biomedical applications. Chemical Society Reviews, 41(7), 2590-2605.
78. Li, Y., Fu, Z. Y., & Su, B. L. (2012). Hierarchically structured porous materials for energy conversion and storage. Advanced Functional Materials, 22(22), 4634-4667.
79. Li, W., Liu, J., & Zhao, D. (2016). Mesoporous materials for energy conversion and storage devices. Nature Reviews Materials, 1(6), 1-17.
80. Li, Y., Li, R., Hu, H., Zhang, K., & Han, P. (2020). Photonic crystal films with high reflectance based on mesoporous silica in the extreme ultraviolet range. Optics Communications, 474, 126110.
81. Liang, J., Liang, Z., Zou, R., & Zhao, Y. (2017). Heterogeneous catalysis in zeolites, mesoporous silica, and metal–organic frameworks. Advanced Materials, 29(30), 1701139.
82. Lidin, S. (1990). Some results of the bonnet transformation. Le Journal de Physique Colloques, 51(C7), C7-237.
83. Linton, P., Rennie, A. R., Zackrisson, M., & Alfredsson, V. (2009). In situ observation of the genesis of mesoporous silica SBA-15: Dynamics on length scales from 1 nm to 1 μm. Langmuir, 25(8), 4685-4691.
84. Liu, S., Lu, L., Yang, Z., Cool, P., & Vansant, E. F. (2006). Further investigations on the modified Stöber method for spherical MCM-41. Materials chemistry and physics, 97(2-3), 203-206.
85. Lord, E. A., & Mackay, A. L. (2003). Periodic minimal surfaces of cubic symmetry. Current Science, 346-362.
86. Lüdtke , S., Adam, T., & Unger, K. K. (1997). Application of 0.5-μm porous silanized silica beads in electrochromatography. Journal of Chromatography A, 786(2), 229-235.
87. Luo, H., Jiang, K., Liang, X., Hua, C., Li, Y., & Liu, H. (2019). Insights into morphological transition of Pluronic P123 micelles as a function of gallate. Colloids and Surfaces A: Physicochemical and Engineering Aspects, 572, 221-229.
88. Luzzati, V., & Spegt, P. A. (1967). Polymorphism of lipids. Nature, 215(5102), 701-704.
89. Luzzati, V., Tardieu, A., & Gulik-Krzywicki, T. (1968). Polymorphism of lipids. Nature, 217(5133), 1028-1030.
90. Luzzati, V., Tardieu, A., Gulik-Krzywicki, T., Rivas, E., & Reiss-Husson, F. (1968). Structure of the cubic phases of lipid–water systems. Nature, 220(5166), 485-488.
91. Mariani, P., Luzzati, V., & Delacroix, H. (1988). Cubic phases of lipid-containing systems: Structure analysis and

biological implications. Journal of molecular biology, 204(1), 165-189.
92. Mariani, P., Amaral, L. Q., Saturni, L., & Delacroix, H. (1994). Hexagonal-cubic phase transitions in lipid containing systems: epitaxial relationships and cylinder growth. Journal de Physique II, 4(8), 1393-1416.
93. Martin, T., Galarneau, A., Di Renzo, F., Fajula, F., & Plee, D. (2002). Morphological control of MCM-41 by pseudomorphic synthesis. Angewandte Chemie, 114(14), 2702-2704.
94. Mertins, O., Mathews, P. D., & Angelova, A. (2020). Advances in the Design of Ph-Sensitive Cubosome Liquid Crystalline Nanocarriers for Drug Delivery Applications. Nanomaterials 2020, 10 (5), 963.
95. Mezzenga, R., Seddon, J. M., Drummond, C. J., Boyd, B. J., Schröder-Turk, G. E., & Sagalowicz, L. (2019). Nature-Inspired Design and Application of Lipidic Lyotropic Liquid Crystals. Advanced Materials, 31(35), 1900818.
96. Mitchell, D. J., Tiddy, G. J., Waring, L., Bostock, T., & McDonald, M. P. (1983). Phase behaviour of polyoxyethylene surfactants with water. Mesophase structures and partial miscibility (cloud points). Journal of the Chemical Society, Faraday Transactions 1: Physical Chemistry in Condensed Phases, 79(4), 975-1000.
97. Miyasaka, K., Garcia Bennett, A., Han, L., Han, Y., Xiao, C., Fujita, N., Castle, T., Sakamoto, Y., Che, S., & Terasaki, O. (2012). The role of curvature in silica mesoporous crystals. Interface Focus, 2(5), 634-644.
98. Monnier, A., Schuth, F., Huo, Q., Kumar, D., Margolese, D., Maxwell, R. S., Stucky, G. D., Krishnamurty, M., Petroff, P., Firouzi, A., Janicke, M., & Chmelka, B. F. (1993). Cooperative formation of inorganic-organic interfaces in the synthesis of silicate mesostructures. Science, 261(5126), 1299-1303.
99. Nagaraj, M. (2020). Liquid Crystals Templating. Crystals, 10, 648.
100. Nakazumi, T., & Hara, Y. (2017). Influence of thickness of alkyl-silane coupling agent coating on separation of small DNA fragments in capillary gel electrophoresis. In IOP Conference Series: Materials Science and Engineering (Vol. 242, No. 1, p. 012034). IOP Publishing.
101. Niculescu, V. C. (2020). Mesoporous silica nanoparticles for bio-applications. Frontiers in Materials, 7, 36.
102. Neto, A. M. F., & Salinas, S. R. (2005). The physics of lyotropic liquid crystals: phase transitions and structural properties (Vol. 62). OUP Oxford.
103. Nozieres, P., Pistolesi, F., & Balibar, S. (2001). Steps and facets at the surface of soft crystals. The European Physical Journal B-Condensed Matter and Complex Systems, 24(3), 387-394.
104. Ojeda-López, R., Domínguez-Ortiz, A., Felipe, C., Cervantes-Uribe, A., Pérez-Hermosillo, I. J., & Esparza-Schulz, J. M. (2021). Isosteric enthalpy behavior of CO2 adsorption on micro-mesoporous materials: carbon microfibers (CMFs), SBA-15, and amine-functionalized SBA-15. Journal of Composites Science, 5(4), 102.
105. Omer, L., Ruthstein, S., Goldfarb, D., & Talmon, Y. (2009). High-resolution cryogenic-electron microscopy reveals details of a hexagonal-to-bicontinuous cubic phase transition in mesoporous silica synthesis. Journal of the American Chemical Society, 131(34), 12466-12473.
106. Paccamiccio, L., Pisani, M., Spinozzi, F., Ferrero, C., Finet, S., & Mariani, P. (2006). Pressure effects on lipidic direct phases: the dodecyl trimethyl ammonium chloride− water system. The Journal of Physical Chemistry B, 110(25), 12410-12418.
107. Pérez-Sánchez, G., Gomes, J. R. B., & Jorge, M. (2013). Modeling Self-Assembly of Silica/Surfactant Mesostructures in the Templated Synthesis of Nanoporous Solids. Langmuir, 29, 2387– 2396.
108. Pérez-Sánchez, G., Chien, S.-C., Gomes, J. R. B., Cordeiro, M. N. D. S., Auerbach, S. M., Monson, P. A., & Jorge, M. (2016). Multiscale Model for the Templated Synthesis of Mesoporous Silica: The Essential Role of Silica Oligomers. Chem. Mater., 28, 2715– 2727.
109. Perroni, D. V., Baez-Cotto, C. M., Sorenson, G. P., & Mahanthappa, M. K. (2015). Linker length-dependent control of gemini surfactant aqueous lyotropic gyroid phase stability. The Journal of Physical Chemistry Letters, 6(6), 993-998.
110. Pieranski, P. (2011). Faceting of Soft Crystals. In Advances in Planar Lipid Bilayers and Liposomes (Vol. 14, pp. 1-43). Academic Press.
111. Popescu-Pampu, P. (2016). What is the Genus? Springer Verlag. ISBN 978-3-319-42312-8.
112. Qiu, H., & Caffrey, M. (2000). The phase diagram of the monoolein/water system: metastability and equilibrium aspects. Biomaterials, 21(3), 223-234.
113. Rançon, Y., & Charvolin, J. (1987). Displacement disorder in a liquid crystalline phase with cubic symmetry. Journal de physique, 48(6), 1067-1073.
114. Roucher, A., Emo, M., Vibert, F., Stébé, M. J., Schmitt, V., Jonas, F., Backov R. & Blin, J. L. (2019). Investigation of mixed ionic/nonionic building blocks for the dual templating of macro-mesoporous silica. Journal of colloid and interface science, 533, 385-400.
115. Roucher, A., Bentaleb, A., Laurichesse, E., Dourges, M. A., Emo, M., Schmitt, V., Blin, J. L. & Backov, R. (2018). First macro-mesocellular silica SBA-15-Si (HIPE) Monoliths: conditions for obtaining self-standing materials. Chemistry of Materials, 30(3), 864-873.
116. Ruthstein, S., Frydman, V., Kababya, S., Landau, M., & Goldfarb, D. J. (2003). Study of the formation of the mesoporous material SBA-15 by EPR spectroscopy. The Journal of Physical Chemistry B, 107(8), 1739-1748.
117. Ruthstein, S., Schmidt, J., Kesselman, E., Talmon, Y., & Goldfarb, D. J. (2006). Resolving intermediate solution structures during the formation of mesoporous SBA-15. Journal of the American Chemical Society, 128(10), 3366-3374.
118. Sakamoto, Y., Diaz, I., Terasaki, O., Zhao, D., Perez-Pariente, J., Kim, J. M., & Stucky, G. D. (2002). Three-dimensional cubic mesoporous structures of SBA-12 and related materials by electron crystallography. The Journal of Physical Chemistry B, 106(12), 3118-3123.
119. Sakya, P., Seddon, J. M., Templer, R. H., Mirkin, R. J., & Tiddy, G. J. T. (1997). Micellar cubic phases and their structural relationships: The nonionic surfactant system C12EO12/water. Langmuir, 13(14), 3706-3714.
120. Sasidharan, M., & Nakashima, K. (2014). Core–shell–corona polymeric micelles as a versatile template for synthesis of

inorganic hollow nanospheres. Accounts of chemical research, 47(1), 157-167.
121. Schwarz, H. (1865). Über Minimalflächen. Monatsber. Berlin Akad., April 1865; Gesammelte Mathematische Abhandlungen, Springer, Berlin, 1890, vol. 1.
122. Schoen, A. H. (1970). Infinite periodic minimal surfaces without self-intersections (No. C-98). NASA Technical Notes.
123. Scriven, L. E. (1976). Equilibrium bicontinuous structure. Nature 263, 123–5.
124. Severs, N. J. (2007). Freeze-fracture electron microscopy. Nature protocols, 2(3), 547-576.
125. Sharma, M. K., & Shah, D. O. (1985). Introduction to macro- and microemulsions. Macro- and Microemulsions, Chapter 1, pp 1-18. ACS Symposium Series Vol. 272, ISBN13: 9780841208964 eISBN: 9780841211025.
126. Shearman, G. C., Ces, O., Templer, R. H., & Seddon, J. M. (2006). Inverse lyotropic phases of lipids and membrane curvature. Journal of Physics: Condensed Matter, 18(28), S1105.
127. Shirwaiker, R. A., Purser, M. F., & Wysk, R. A. (2014). Scaffolding hydrogels for rapid prototyping based tissue engineering. In Rapid Prototyping of Biomaterials (pp. 176-200). Woodhead Publishing.
128. Seddon, J. M., Zeb, N., Templer, R. H., McElhaney, R. N., & Mannock, D. A. (1996). An Fd 3 m lyotropic cubic phase in a binary glycolipid/water system. Langmuir, 12(22), 5250-5253.
129. Siegel, D. P. (1986). Inverted micellar intermediates and the transitions between lamellar, cubic, and inverted hexagonal lipid phases. II. Implications for membrane-membrane interactions and membrane fusion. Biophysical journal, 49(6), 1171-1183.
130. Silverstein, M. S. (2014). PolyHIPEs: Recent advances in emulsion-templated porous polymers. Progress in Polymer Science, 39(1), 199-234.
131. Slowing, I. I., Vivero-Escoto, J. L., Trewyn, B. G., & Lin, V. S. Y. (2010). Mesoporous silica nanoparticles: structural design and applications. Journal of Materials Chemistry, 20(37), 7924-7937.
132. Soni, S. S., Brotons, G., Bellour, M., Narayanan, T., & Gibaud, A. (2006). Quantitative SAXS analysis of the P123/water/ethanol ternary phase diagram. The journal of physical chemistry B, 110(31), 15157-15165.
133. Sorenson, G. P., & Mahanthappa, M. K. (2015). Structure versus Function in Polycontinuous Network Phases: What's in a name? in Reply to the 'Comment on "Discovery of a tetracontinuous, aqueous lyotropic network phase with unusual 3D-hexagonal symmetry"'by G. Schröder-Turk, M. Fischer and S. Hyde. Soft Matter, 11(6), 1228-1230.
134. Sparavigna, A.C. (2022). Lyotropic liquid crystals as templates for mesoporous silica materials. SSRN, DOI: 10.2139/ssrn.4285677
135. Sparavigna AC. (2022). Liquid crystal templates of mesoporous silica materials. ChemRxiv. Cambridge: Cambridge Open Engage.
136. Sparavigna, A. C. (2023). Water in Pores: The Gibbs-Thomson Effect. SSRN, DOI: 10.2139/ssrn.4349640
137. Stöber, W., Fink, A., & Bohn, E. (1968). Controlled growth of monodisperse silica spheres in the micron size range. Journal of colloid and interface science, 26(1), 62-69.
138. Sun, M. H., Huang, S. Z., Chen, L. H., Li, Y., Yang, X. Y., Yuan, Z. Y., & Su, B. L. (2016). Applications of hierarchically structured porous materials from energy storage and conversion, catalysis, photocatalysis, adsorption, separation, and sensing to biomedicine. Chemical society reviews, 45(12), 3479-3563.
139. Tan, C., Hosseini, S. F., & Jafari, S. M. (2022). Cubosomes and hexosomes as novel nanocarriers for bioactive compounds. Journal of Agricultural and Food Chemistry, 70(5), 1423-1437.
140. Teubner, M., & Strey, R. (1987). Origin of the scattering peak in microemulsions. The Journal of Chemical Physics, 87(5), 3195-3200.
141. Thibaut, A., Misselyn-Bauduin, A. M., Broze, G., & Jérôme, R. (2000). Adsorption of poly (vinylpyrrolidone)/surfactant (s) mixtures at the silica/water interface: a calorimetric investigation. Langmuir, 16(25), 9841-9849.
142. Tran, N., Zhai, J., Conn, C. E., Mulet, X., Waddington, L. J., & Drummond, C. J. (2018). Direct visualization of the structural transformation between the lyotropic liquid crystalline lamellar and bicontinuous cubic mesophase. The Journal of Physical Chemistry Letters, 9(12), 3397-3402.
143. Tresset, G. (2009). The multiple faces of self-assembled lipidic systems. PMC biophysics, 2(1), 1-25.
144. Tsitsilianis, C., Voulgaris, D., Štěpánek, M., Podhájecká, K., Procházka, K., Tuzar, Z., & Brown, W. (2000). Polystyrene/poly (2-vinylpyridine) heteroarm star copolymer micelles in aqueous media and onion type micelles stabilized by diblock copolymers. Langmuir, 16(17), 6868-6876.
145. Vallet-Regí, M., Schüth, F., Lozano, D., Colilla, M., & Manzano, M. (2022). Engineering mesoporous silica nanoparticles for drug delivery: where are we after two decades?. Chemical Society Reviews, 51, 5365-5451.
146. Vallet-Regi, M., Rámila, A., Del Real, R. P., & Pérez-Pariente, J. (2001). A new property of MCM-41: drug delivery system. Chemistry of Materials, 13(2), 308-311.
147. Van Der Voort, P., Morey, M., Stucky, G. D., Mathieu, M., & Vansant, E. F. (1998). Creation of VO_x Surface Species on Pure Silica MCM-48 Using Gas-Phase Modification with $VO(acac)_2$. The Journal of Physical Chemistry B, 102(3), 585-590.
148. Vertogen, G., & De Jeu, W. H. (2012). Thermotropic liquid crystals, fundamentals (Vol. 45). Springer Science & Business Media.
149. Vincent, B. (2014). McBain and the centenary of the micelle. Advances in colloid and interface science, 203, 51-54.
150. Vinu, A., Miyahara, M., Sivamurugan, V., Mori, T., & Ariga, K. (2005). Large pore cage type mesoporous carbon, carbon nanocage: a superior adsorbent for biomaterials. Journal of Materials Chemistry, 15(48), 5122-5127.
151. Vivero-Escoto, J. L., Slowing, I. I., Trewyn, B. G., & Lin, V. S. Y. (2010). Mesoporous silica nanoparticles for intracellular controlled drug delivery. Small, 6(18), 1952-1967.
152. Wan, Y., & Zhao, D. (2007). On the controllable soft-templating approach to mesoporous silicates. Chemical Reviews, 107(7), 2821-2860.
153. Wawrzyńczak, A., Jarmolińska, S., & Nowak, I. (2022). Nanostructured KIT-6 materials functionalized with sulfonic groups for catalytic purposes. Catalysis Today, 397, 526-539.

154. Wei, T. C., & Hillhouse, H. W. (2007). Mass transport and electrode accessibility through periodic self-assembled nanoporous silica thin films. Langmuir, 23(10), 5689-5699.
155. Winsor, P. A. (1968). Binary and multicomponent solutions of amphiphilic compounds. Solubilization and the formation, structure, and theoretical significance of liquid crystalline solutions. Chemical reviews, 68(1), 1-40.
156. Wu, L., Li, Y., Fu, Z., & Su, B. L. (2020). Hierarchically structured porous materials: Synthesis strategies and applications in energy storage. National Science Review, 7(11), 1667-1701.
157. Xu, R., Pang, W., Yu, J., Huo, Q., & Chen, J. (2009). Chemistry of zeolites and related porous materials: synthesis and structure. John Wiley & Sons.
158. Xu, C., Lei, C., Wang, Y., & Yu, C. (2022). Dendritic mesoporous nanoparticles: structure, synthesis and properties. Angewandte Chemie, 134(12), e202112752.
159. Yablonovitch, E. (1987). Inhibited spontaneous emission in solid-state physics and electronics, Phys. Rev. Lett. 58, 2059–2062.
160. Yaghmur, A., Laggner, P., Zhang, S., & Rappolt, M. (2007). Tuning curvature and stability of monoolein bilayers by designer lipid-like peptide surfactants. PLoS One, 2(5), e479.
161. Yanagisawa, T., Shimizu, T., Kuroda, K., & Kato, C. (1990). The preparation of alkyltrimethylammonium–kanemite complexes and their conversion to microporous materials. Bulletin of the Chemical Society of Japan, 63(4), 988-992.
162. Yokoi, T., Yoshitake, H., & Tatsumi, T. (2003). Synthesis of anionic-surfactant-templated mesoporous silica using organoalkoxysilane-containing amino groups. Chemistry of materials, 15(24), 4536-4538.
163. Zhang, G., Chen, X., Zhao, Y., Ma, F., Jing, B., & Qiu, H. (2008). Lyotropic liquid-crystalline phases formed by Pluronic P123 in ethylammonium nitrate. The Journal of Physical Chemistry B, 112(21), 6578-6584.
164. Zhao, X. S., Lu, G. Q., Whittaker, A. K., Millar, G. J., & Zhu, H. Y. (1997). Comprehensive study of surface chemistry of MCM-41 using 29Si CP/MAS NMR, FTIR, pyridine-TPD, and TGA. The Journal of Physical Chemistry B, 101(33), 6525-6531.
165. Zhao, D., Feng, J., Huo, Q., Melosh, N., Fredrickson, G. H., Chmelka, B. F., & Stucky, G. D. (1998). Triblock copolymer syntheses of mesoporous silica with periodic 50 to 300 angstrom pores. science, 279(5350), 548-552.
166. Zholobenko, V. L., Khodakov, A. Y., Impéror-Clerc, M., Durand, D., & Grillo, I. (2008). Initial stages of SBA-15 synthesis: An overview. Advances in Colloid and Interface Science, 142(1-2), 67-74.
167. Zeng, X., Poppe, S., Lehmann, A., Prehm, M., Chen, C., Liu, F., Lu, H., Ungar, G., & Tschierske, C. (2019). A Self-Assembled Bicontinuous Cubic Phase with a Single-Diamond Network. Angewandte Chemie, 131(22), 7453-7457.
168. Zhu, Y., Shi, J., Shen, W., Chen, H., Dong, X., & Ruan, M. (2005). Preparation of novel hollow mesoporous silica spheres and their sustained-release property. Nanotechnology, 16(11), 2633.